How Far Can Proteins Bend the FeCO Unit? Distal Polar and Steric Effects in Heme Proteins and Models†

Gigi B. Ray,‡,§ Xiao-Yuan Li,‖ James A. Ibers,⊥ Jonathan L. Sessler,+ and Thomas G. Spiro*,§

Contribution from the Departments of Chemistry, Princeton University, Princeton, New Jersey 08544, Hong Kong University of Science and Technology, Clear Water Bay, Kowloon, Hong Kong, and Northwestern University, Evanston, Illinois 60208-3113, and Department of Chemistry and Biochemistry, University of Texas, Austin, Texas 78712-1167

Received April 1, 1993•

Abstract: Resonance Raman (RR) spectra are reported for structurally defined CO adducts of two sterically constrained Fe^{II} porphyrins: PocPiv, in which three of the pivaloylamino pickets of "picket fence" porphyrin (5,10,15,20-tetrakis-[*o*-(pivaloylamino)phenyl]porphyrin) are attached to a benzene cap by single methylene groups, and C_2-Cap, in which a benzene cap is attached by carboxylate links and a pair of methylene groups to the four hydroxyl groups of 5,10,15,20-tetrakis(*o*-hydroxyphenyl)porphyrin. Although the X-ray crystal structures of the two adducts show very similar FeCO geometries, involving a small amount of bending and tilting, their vibrational frequencies and RR enhancement patterns are very different. Relative to unconstrained porphyrins, the C–O and Fe–C stretching (ν_{CO} and ν_{FeC}) frequencies show increased Fe→CO back-bonding for PocPiv but decreased back-bonding for C_2-Cap. The Fe–C–O bending mode (δ_{FeCO}) is activated for PocPiv but not for C_2-Cap. These contrasting patterns can be attributed to the different polar interactions of the bound CO in the two adducts. In the PocPiv adduct, the O atom is in close contact with one of the amide NH groups; this positive polar interaction increases back-bonding. In the C_2-Cap adduct, the linker arms have ester and ether, rather than amide, groups and there is a close contact between the CO and the benzene π-cloud; this negative polar environment decreases back-bonding. In addition the cap interaction may compress the FeC bond in C_2-Cap, as evidenced by a ν_{FeC} frequency elevation from the value expected on the basis of the back-bonding decrease. The extensive vibrational data on CO adducts of heme proteins and on sterically constrained synthetic porphyrins are reexamined in the light of these results. Essentially all of the data are consistent with expected polar effects in the binding pocket. Positive distal polar interactions (1) increase ν_{FeC} and decrease ν_{CO} along a back-bonding correlation that depends only on the nature of the trans axial ligand, (2) diminish the intensity of the ν_{FeC} RR band (attributed to a reduction in the Fe–C bond displacement between the ground and excited states), and (3) activate the FeCO bending mode (by perturbing the 4-fold electronic symmetry via off-axis interactions). A recent proposal that the RR band usually assigned to δ_{FeCO} actually arises from the bending mode overtone is discussed and is rejected on the basis of comparisons with transition metal carbonyls for which thorough vibrational analyses are available. Elimination of positive polar interactions reverses all three of these effects. The energetics of the small FeCO distortions seen in the PocPiv and C_2-Cap adducts are evaluated and are found to account for most of the CO affinity reductions of these constrained porphyrins. The polar interactions appear to contribute only a small part of the overall energy, even though they have a dominant effect on the vibrational frequency variation. It is argued that large sterically-induced FeCO distortions are precluded by the prohibitive energy cost, especially in proteins, where the available steric force is limited by the conformational flexibility of the polypeptide. Somewhat greater FeCO bending than has so far been observed in models is indicated for one of the substates, A_3, of the CO adduct of myoglobin. This effect is suggested to arise from a donor interaction with an imidazole lone pair, consistent with the distal histidine tautomer determined by neutron diffraction. Even in this case, however, the IR frequency precludes FeCO angles as small as 120–140°, values reported from early determinations of MbCO crystal structures containing disordered CO. The dominant MbCO substates in solution, $A_{1,2}$, are indicated to have a significant polar interaction with the distal histidine, in the alternate tautomer to the one seen in the neutron structure, and probably have nearly linear FeCO units, consistent with the most recent X-ray structure determination of a nondisordered crystal form.

Introduction

The carbon monoxide (CO) molecule plays a central role in studies of heme protein structure and function. It serves as a surrogate for the physiological reactant, dioxygen (O_2); both ligands bind to heme iron(II), forming low-spin complexes, and they induce much the same changes in the protein structure. For example, both ligands convert hemoglobin from the T (tense) to the R (relaxed) quaternary structure. The CO adduct, being unreactive, is easier to study, and its high quantum yield for photodissociation has been extensively utilized in studies of ligand rebinding and of the time evolution of the protein structure in response to deligation. Moreover, the vibrational frequencies of the FeCO unit, available from resonance Raman (RR) and infrared (IR) spectroscopy,[1,2] and the ^{13}C and ^{17}O NMR chemical

* Author to whom correspondence should be addressed.

† Abbreviations used in paper: OEP = octaethylporphyrin; TPP = tetraphenylporphyrin; Deut = deuteroheme; TSMP = tetrakis(*p*-sulfonatomesityl)porphyrin; TPivP = picket fence porphyrin; SP-13 to SP-15 and heme-5 = strapped and unstrapped octaethyl hemes; Piv_2C_n = bis-picket, basket handle (n = 8–12) porphyrins; α-PocPiv, α-MedPoc, and α-TalPoc = small, medium, and tall pocket porphyrins; PPIX and PPDME = protoporphyrin-IX and its dimethyl ester; APC = adamantane hemin 6,6-cyclophane; TSPP = tetrakis-(*p*-sulfonatophenyl)porphyrin; C_2-Cap and C_3-Cap = small and medium (ether/ester linked) capped porphyrins; Anth66 and Anth77 = anthracene hemin 6,6-cyclophane and 7,7-analog; OCCO = diether-linked capped porphyrin; NMeIm = *N*-methylimidazole; 1,2-Me_2Im = 1,2-dimethylimidazole; 4MeIm = 4-methylimidazole; 2MeImH = 2-methylimidazole.

‡ Present address: Department of Tumor Cell Biology, St. Jude Children's Research Hospital, Memphis, TN 38105.

§ Princeton University.

‖ Hong Kong University of Science and Technology.

⊥ Northwestern University.

+ University of Texas.

• Abstract published in *Advance ACS Abstracts*, December 1, 1993.

0002-7863/94/1516-0162$04.50/0

shifts[3-5] are useful indicators of ligand interactions with the residues lining the heme binding pocket.

Still, CO and O_2 differ significantly in their electronic structure and in their mode of binding. The binding affinities differ, and the discrimination factor between the two ligands varies with the protein and between proteins and model complexes.[6] The determinants of binding affinity have been vigorously debated. The FeCO unit prefers a linear geometry, in order to maximize Fe $d_\pi \rightarrow$ CO π^* back-bonding, while the FeO_2 unit, with two extra electrons, is strongly bent. Initial attention focused on this bent vs linear dichotomy and on the possibility that CO binding is selectively inhibited by steric interactions that impede upright binding.[7,8] More recently, the emphasis has shifted to polar interactions in the binding pocket.[9] Electron transfer from Fe to the bound ligand is greater for O_2, which has lower lying π^* orbitals than CO. The developing negative charge is more strongy stabilized by H-bonding groups, positive charges, or the positive end of dipoles, in the case of O_2.

Much of the research on steric effects was stimulated by early neutron[10] and X-ray[11] crystal structure determinations of the CO adduct of sperm whale myoglobin, MbCO, in which it was reported that the CO, although disordered, adopts strongly bent conformations, with FeCO angles of 120–141°. Several porphyrins have been synthesized with covalently linked superstructures that are designed to hinder upright binding of the CO. High-resolution X-ray crystal structures are now available for CO adducts of two of these sterically constrained porphyrins, and both show only small degrees of tilting and bending.[12,13] Moreover, a very recent X-ray determination[14] of a new MbCO crystal form, in which the CO is not disordered, gives a FeCO angle of 169°; similar values have earlier been reported for HbCO.[15]

In the present study, RR spectra are reported for the two structurally characterized sterically-constrained FeCO porphyrin adducts, PocPiv,[12] in which three of the pivaloylamino pickets of "picket fence" porphyrin (tetrakis[*o*-(pivaloylamino)phenyl]-porphyrin) are attached to a benzene cap by single methylene groups (Figure 1), and C_2-Cap,[13] in which a benzene cap is attached by carboxylate links and a pair of methylene groups to the four hydroxyl groups of tetrakis(*o*-hydroxyphenyl)porphyrin (Figure 2). They show very different FeCO vibrational frequencies and RR enhancement patterns. Since the FeCO distortions are similar, these differences must have an electronic basis, which can readily be traced to the different interactions of the CO: a close contact with an amide NH group in the PocPiv adduct but with the benzene ring in C_2-Cap.

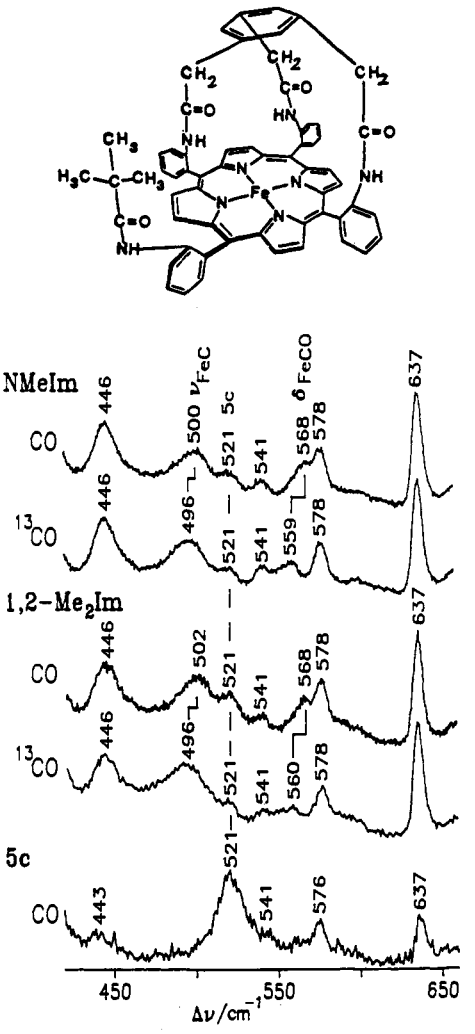

Figure 1. Resonance Raman spectra of Fe$^{II}\alpha$-PocPiv(L)(CO) adducts in methylene chloride, obtained with 413.1-nm excitation, with 6-cm^{-1} spectral slit widths, and with 14-s accumulation at 0.5-cm^{-1} increments using a scanning monochromator. The sixth ligand (L) is *N*-methylimidazole in the top two spectra, 1,2-dimethylimidazole in the middle two, and absent in the bottom spectrum, which is of the five-coordinate (5c) Fe^{II}(CO) adduct. The solid lines show carbon monoxide isotope shifts between natural abundance CO and ^{13}CO in the ν_{FeC} and δ_{FeCO} modes. The dashed line marks a residual 5c component, present in all the spectra. The chemical structure of Feα-PocPiv is shown at the top.

Until now sterically constrained porphyrins have all shown elevated Fe–C stretching frequencies and RR activation of the ordinarily inactive FeCO bending mode.[16,17] These characteristics are shared by MbCO[18] and have been taken to be indicators of FeCO distortion.[16] We find them to be shared by the PocPiv adduct but *not* by the C_2-Cap adduct. The new results on PocPiv and C_2-Cap permit us to reinterpret the earlier spectra as indicative of distal polar interactions. Indeed the vibrational spectra of the CO adducts of a wide range of iron porphyrins and heme proteins, including, it is argued below, mutant myoglobins and hemoglobins, peroxidases, cytochrome oxidase, and cytochrome P450, can be understood on the basis of variable distal polar interactions. In most cases there is no indication of significant FeCO distortion. Oldfield and co-workers have likewise concluded that distal polar interactions provide a satisfactory explanation of the available ^{13}C and ^{17}O NMR data on heme protein CO adducts.[3-5]

(1) Kerr, E.; Yu, N.-T. In *Biological Applications of Raman Spectroscopy, Vol 3: Resonance Raman Spectra of Heme and Metalloproteins*; Spiro, T. G., Ed.; Wiley-Interscience: New York, 1988; pp 39–95.
(2) Yu, N.-T. *Methods Enzymol.* **1986**, *130*, 350–409.
(3) Park, K. D.; Guo, K.; Adebodun, F.; Chiu, M. L.; Sligar, S. G.; Oldfield, E. *Biochemistry* **1991**, *30*, 2333–2347.
(4) Augspurger, J. D.; Dykstra, C. E.; Oldfield, E. *J. Am. Chem. Soc.* **1991**, *113*, 2447–2451.
(5) Oldfield, E.; Guo, K.; Augspurger, J. D.; Dykstra, C. E. *J. Am. Chem. Soc.* **1991**, *113*, 7537–7541.
(6) Traylor, T. G. *Acc. Chem. Res.* **1981**, *14*, 102–109.
(7) Collman, J. P.; Brauman, J. I.; Iverson, B. L.; Sessler, J. L.; Morris, R. M.; Gibson, Q. H. *J. Am. Chem. Soc.* **1983**, *105*, 3052–3064.
(8) (a) Collman, J. P.; Brauman, J. I.; Collins, T. J.; Iverson, B. L.; Lang, G.; Pettman, R. B.; Sessler, J. L.; Walters, M. A. *J. Am. Chem. Soc.* **1983**, *105*, 3038–3052. (b) Collman, J. P.; Brauman, J. I.; Halbert, T. R.; Suslick, K. S. *Proc. Natl. Acad. Sci. U.S.A.* **1976**, *73*, 3333–3337.
(9) Traylor, T. G.; Koga, N.; Deardurff, L. A. *J. Am. Chem. Soc.* **1985**, *107*, 6504–6510.
(10) (a) Cheng, X.; Schoenborn, B. *J. Mol. Biol.* **1991**, *220*, 381–399. (b) Cheng, X.; Schoenborn, B. P. *Acta Crystallogr.* **1990**, *B46*, 195–208. (c) Hanson, J. C.; Schoenborn, B. P. *J. Mol. Biol.* **1981**, *153*, 117–146. (d) Norvell, J. C.; Nunes, A. C.; Schoenborn, B. P. *Science* **1975**, *190*, 568–570.
(11) Kuriyan, J.; Wilz, S.; Karplus, M.; Petsko, G. A. *J. Mol. Biol.* **1986**, *192*, 133–154.
(12) Kim, K.; Fettinger, J.; Sessler, J. L.; Cyr, M.; Hugdahl, J.; Collman, J. P.; Ibers, J. A. *J. Am. Chem. Soc.* **1989**, *111*, 403–405.
(13) Kim, K.; Ibers, J. A. *J. Am. Chem. Soc.* **1991**, *113*, 6077–6081.
(14) Quillin, M. L.; Arduini, R. M.; Olson, J. S.; Phillips, G. N., Jr. *J. Mol. Biol.* **1993**, *234*, 140–155.
(15) Derewenda, Z.; Dodson, G.; Emsley, P.; Harris, D.; Nagai, K.; Perutz, M. F.; Renaud, J. P. *J. Mol. Biol.* **1990**, *211*, 515–519.
(16) Yu, N.-T.; Kerr, E. A.; Ward, B.; Chang, C. K. *Biochemistry* **1983**, *22*, 4534–4540.
(17) Desbois, A.; Momenteau, M.; Lutz, M. *Inorg. Chem.* **1989**, *28*, 825–834.
(18) Tsubaki, M.; Srivastava, R. B.; Yu, N.-T. *Biochemistry* **1982**, *21*, 1132–1140.

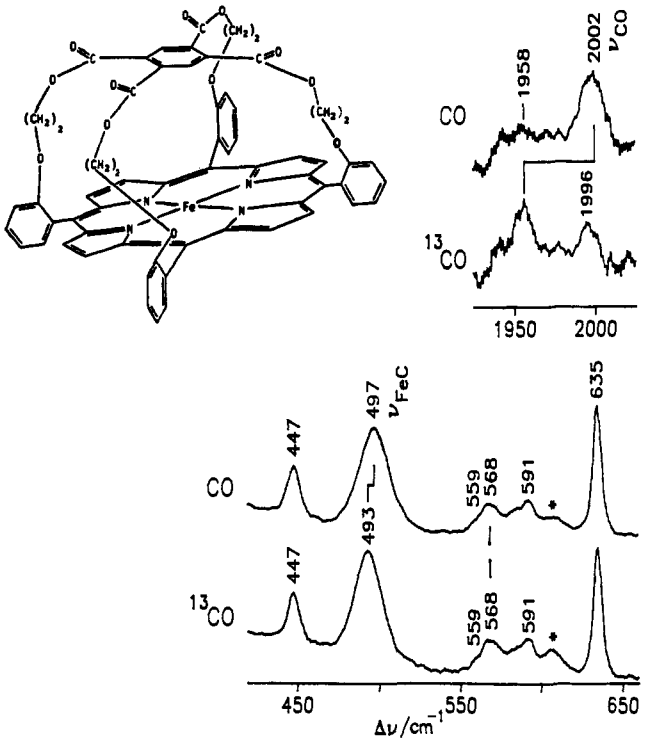

Figure 2. Resonance Raman spectra of $Fe^{II}C_2$-Cap(NMeIm)(CO) in benzene, obtained with 413.1-nm excitation, using a 2400 groove/mm grating in the spectrograph, with 60-μm slits and 20-min accumulation (diode array detection). The upper two traces show the high-frequency (1925–2025 cm^{-1}) region, while the lower two spectra show the low-frequency (420–660 cm^{-1}) region. Solid lines mark CO isotope shifts in the ν_{CO} and ν_{FeC} modes. The dashed line shows that the 568-cm^{-1} band lacks isotope sensitivity and is therefore a porphyrin mode rather than δ_{FeCO}. The asterisk indicates a solvent (benzene) band at 606 cm^{-1}. The chemical structure of FeC_2-Cap is shown at the top.

We have estimated FeCO distortion energies from the available force constants and find that they account for most of the decreased binding energies of PocPiv and C_2-Cap, relative to an uncapped analog. The energies associated with the electronic interactions that determine the vibrational frequencies are evidently small in comparison. We conclude that steric factors can inhibit CO binding without producing large distortions of the adduct geometry. Indeed the energy required for large distortions is prohibitive and would simply inhibit binding completely.

The situation in MbCO is complicated by the coexistence of several substates. We discuss evidence that the main substates in solution, $A_{1,2}$, are likely to be nearly linear and subject to a polar interaction with the nearby distal histidine side chain but that a minority substate, A_3, which becomes more populated upon crystallization from ammonium sulfate, has a somewhat more distorted geometry. This distortion may result from a donor interaction with a lone pair on the distal histidine, which is adjacent to the CO in the tautomer seen in the neutron crystal structure.[10] Even in this case, however, the CO stretching frequency is too high to permit FeCO angles in the 120–140° range.

Experimental Methods

Iron(III) tetrakis(4-sulfonatomesityl)porphyrin, sodium salt [Fe^{III}-TSMP], iron(III) tetrakis(4-sulfonatophenyl)porphyrin, sodium salt [Fe^{III}-TSPP], and *m*-tetrakis($\alpha,\alpha,\alpha,\alpha$-*o*-pivaloylaminophenyl)porphyrin (H_2-TPivP) were purchased from Mid Century Chemicals, Posen, IL, and used without further purification. Carbon monoxide (CO) gas (CP grade) was purchased from MG Industries, and isotopically labeled ^{13}CO gas (99% enriched, with ca. 10% C^{18}O) was purchased from Cambridge Isotope Laboratories. Anhydrous $FeBr_2$ was purchased from Alfa Products. Activated grade I neutral alumina (Aldrich) was evacuated for 24 h and stored under N_2 prior to use. 4-Methylimidazole (4MeIm), 2-methylimidazole (2MeIm), *N*-methylimidazole (NMeIm), and 1,2-dimethylimidazole (1,2-Me_2Im) were purchased from Sigma. The latter two imidazoles were distilled under reduced pressure to obtain colorless, nonfluorescent material. The following solvents were purchased commercially and distilled under N_2 before use: CH_2Cl_2, MeOH, and piperidine from CaH_2, benzene and toluene from sodium metal, 2,6-lutidine from BaO, and THF from benzophenone/sodium.

An anaerobic RR cell was designed to allow *in situ* preparation of small volumes (350 μL) of reduced, air-sensitive porphyrins. The solution was stirred vigorously with a magnetic stir bar during RR spectroscopy to reduce CO photolysis. The cell design permitted direct measurement of Q-band absorption spectra of 100-200 μM porphyrin solutions. The cell has two parts clamped together at an O-ring joint (size 112) and is mounted above a variable-speed rotating magnet in the RR setup. The lower half of the cell consists of a 8-mm i.d., 1.5-in.-long flat-bottomed Suprasil quartz (Wilmad) tube, fused to a quartz O-ring joint, and containing a snugly fitting $^1/_4$-in. Teflon-covered stirring bar (Spinfin, Chemglass). The upper half of the cell consists of a 2-in. glass tube fused to a glass O-ring joint, which can be sealed at the top with a rubber septum, allowing addition of liquid reductant or gaseous N_2 or CO directly to the sample with a needle. Midway up the tube is a 145° angled Flickit valve (Ace Glass), with an angled Teflon plug and Viton O-ring, which either seals the cell following sample preparation or can be rotated out of the vertical tube to allow additions to the sample. A similar anaerobic absorption cell was designed for UV–vis titrations of Fe^{II}CO porphyrins with imidazoles. It has an optically flat 5-mm quartz spectrophotometric cell (NSG Precision Cells) in the lower half. During sample preparation all anaerobic solution transfers were made with gastight Hamilton syringes (25 μL to 5 mL).

Preparation of six-coordinate (6c) Fe^{II}(L)(CO) porphyrin adducts[19] requires careful control of the imidazole base concentration, because of the varying affinities of imidazoles and CO. We titrated the five-coordinate (5c) Fe^{II}CO adducts of PocPiv and the water-soluble porphyrins with imidazoles to determine the optimal base concentration required to form the desired 6c imidazole–CO adducts. It was observed that as the solvent polarity is increased from benzene to methylene chloride to aqueous buffer, larger amounts of imidazole must be added to form the desired 6c adduct, reflecting enhanced solvation of the imidazole. In sterically constrained porphyrins, since CO and imidazole compete for coordination to the unencumbered (proximal) side, very high (1–3 M) concentrations of imidazole are required to force CO to bind within the distal pocket. All the adducts were characterized initially by absorption spectroscopy between 300 and 800 nm on a 8451A Hewlett-Packard diode-array UV–vis spectrophotometer. The Q-band absorption spectra of the RR samples were obtained directly in the anaerobic RR cell, prior to and immediately following RR spectroscopy, to monitor sample oxidation and integrity.

Purified $H_2\alpha$-PocPiv, 5,10,15-((1,3,5-benzenetriyltriacetyl)tris(α,α,α-*o*-aminophenyl))-20-(α-*o*-pivaloylaminophenyl)porphyrin was prepared by literature methods.[8] Iron(II) was inserted directly into the free-base porphyrin in a N_2 drybox and was handled subsequently in anaerobic cells under a N_2 atmosphere at a vacuum-Schlenk line, in order to avoid air oxidation to iron(III). A 25-mg amount of $H_2\alpha$-PocPiv was metalated as described in ref 8, with the following modifications. In order to minimize heating of the porphyrin, which can cause α- to β-atropisomerization of the fourth untethered picket, hot solvent and excess ferrous bromide were added simultaneously to the free-base porphyrin. The slurry was stirred vigorously and then immediately cooled by evaporating the solvent in a rotary evaporator. After chromatography to remove unreacted $FeBr_2$, the $Fe^{II}\alpha$-PocPiv was evaporated to dryness and stored in a drybox, in the dark. Immediately prior to the RR experiments, $Fe^{II}\alpha$-PocPiv was dissolved in distilled, degassed methylene chloride and the solution was placed in the anaerobic RR cell. After addition of degassed imidazole, the sample was frozen in liquid N_2, and the cell was evacuated and then refilled with 1 atm of CO gas. Upon thawing of the sample, a color change from reddish-brown to bright red[19] indicated formation of $Fe^{II}\alpha$-PocPiv(imidazole)(CO). Absorption and RR titrations of $Fe^{II}\alpha$-PocPiv-(CO) with NMeIm and 1,2-Me_2Im in methylene chloride indicated that only upon addition of greater than 1 M base does the 6c imidazole–CO species predominate; these concentrations are higher than those reported in ref 8 for toluene solutions. Final concentrations used were 150 μM porphyrin and either 1.3 M NMeIm or 1.2 M 1,2-Me_2Im, which yield the following absorption data: $Fe^{II}\alpha$-PocPiv(CO), 420 and 510 nm; $Fe^{II}\alpha$-PocPiv(NMeIm)(CO), 426 and 525 nm; $Fe^{II}\alpha$-PocPiv(1,2-Me_2Im)(CO),

(19) (a) Collman, J. P.; Basolo, F.; Bunnenberg, E.; Collins, T. J.; Dawson, J. H.; Ellis, P. E.; Marrocco, M. L.; Moscowitz, A.; Sessler, J. L.; Szymanski, T. *J. Am. Chem. Soc.* **1981**, *103*, 5636–5648. (b) Collman, J. P.; Brauman, J. I.; Collins, T. J.; Iverson, B. L.; Sessler, J. L. *J. Am. Chem. Soc.* **1981**, *103*, 2450–2452.

426 and 518 nm. Fe^{II} was inserted into H_2TPivP in the same manner as in $H_2\alpha$-PocPiv. RR samples of Fe^{II}TPivP(1,2-Me_2Im)(CO) in methylene chloride were prepared in an analogous way, with 32 mM 1,2-Me_2Im added.

$Fe^{III}C_2$-Cap(Cl), [5,10,15,20-(pyromellitoyltetrakis(*o*-(oxyethoxy)-phenyl))porphyrinato]iron(III) chloride was prepared as described in ref 20a. C_2 refers to the presence of two methylene groups in the cap linker arms. $Fe^{III}C_2$-Cap(Cl) was dissolved in benzene and degassed by flushing with N_2. After addition of an equal volume of degassed aqueous sodium dithionite (~0.6 M), the solution was stirred vigorously for a few minutes whereupon the color changed from brown to reddish-brown, indicating iron reduction. After phase separation, $Fe^{II}C_2$-Cap from the upper benzene layer was transferred into a degassed solution of NMeIm in benzene, containing anhydrous sodium sulfate. The slurry was stirred for a few minutes and then allowed to settle. After the transfer of aliquots of dry $Fe^{II}C_2$-Cap(NMeIm) into the anaerobic RR cells, the samples were frozen and the cell was evacuated and then refilled with 1 atm of CO. When the sample was thawed, a color change to bright red indicated formation of $Fe^{II}C_2$-Cap(NMeIm)(CO), which has λ_{max} at 424, 542, and 580 (sh) nm. Final concentrations used were 170 μM porphyrin and 2.6 M NMeIm.

Fe^{III}OCCO(Cl), [5,10,15,20-((1,2,4,5-benzenetetrayl)tetrakis(*o*-(oxyethoxy)phenyl))porphyrinato]iron(III) chloride, was prepared as described in ref 21. The Fe^{II}OCCO(NMeIm)(CO) adduct in benzene, which has λ_{max} at 410 (sh), 426, 546, 567 (sh), and 611 (sh) nm, was prepared in the same manner as the analogous C_2-Cap complex. The final concentrations used were 150 μM porphyrin and 1 M NMeIm.

The water-soluble porphyrins Fe^{III}TSMP, iron(III) tetrakis(4-sulfonatomesityl)porphyrin, and Fe^{III}TSPP, iron(III) tetrakis(4-sulfonatophenyl)porphyrin, (230 μM) were dissolved in 100 mM phosphate buffer, pH 7, with or without excess imidazole present. The degassed samples were reduced upon anaerobic addition of a minimum amount of degassed aqueous sodium dithionite. CO was flushed over the stirred samples for ~30 min. Fe^{II}TSMP(4MeIm)(CO), with 19 mM 4MeIm present, has λ_{max} at 424, 544, and 583 nm, while in the absence of any base Fe^{II}-TSMP(H_2O)(CO) is formed with λ_{max} at 418 and 540 nm. Because of the lower binding affinity of 2MeIm versus 4MeIm, Fe^{II}TSPP(2MeIm)-(CO) forms upon addition of 250 mM 2MeIm, with λ_{max} at 422, 518 (sh), 532, and 568 nm.

Resonance Raman spectra were obtained with excitation from the 413.1- or 406.7-nm lines of a Kr^+ ion laser (Coherent Innova 100-K3), with a backscattering sampling geometry. Very low laser power (2–5 mW) at the sample, a defocused beam, and rapid stirring of the room-temperature solutions were used to minimize CO photodissociation, as monitored by the ν_4 porphyrin skeletal mode. In the Feα-PocPiv and FeTPivP RR experiments the scattered light was collected and focused into a scanning double monochromator (SPEX 1401) equipped with a cooled photomultiplier tube (RCA) and photon-counting electronics, all under the control of an IBM personal computer. In the FeC_2-Cap, FeTSMP, and FeTSPP experiments the scattered light was focused into a triple monochromator (SPEX 1877) equipped with a diode array optical multichannel detector (PAR 1420) cooled to −22 °C to reduce dark current. Spectra were calibrated with indene and carbon tetrachloride.

Results

1. Small Pocket Porphyrin (PocPiv). Low-frequency (420–660 cm^{-1}) RR spectra obtained with 413.1-nm Soret excitation of three Fe^{II}CO adducts of the α-atropisomer (picket-up) of the small pocket porphyrin (PocPiv) are shown in Figure 1. The pocket superstructure, consisting of a benzene cap attached to three out of four of the porphyrin C_m-phenyl substituents via *o*-amide linker groups and a fourth free pivaloylamino picket (see Figure 1 inset), protects one side of the heme from imidazole ligation.[8] Imidazole is forced to bind on the unhindered (proximal) side, while small ligands such as CO and O_2 can bind within the distal pocket in the presence of an excess of nitrogenous base.[8] As shown in the bottom spectrum in Figure 1, ligation of CO in the absence of imidazole yields a five-coordinate (5c) Fe^{II}PocPiv-(CO) adduct with a strong RR band at 521 cm^{-1} (compare with 526 and 524 cm^{-1} for 5c FeCO adducts of FeTPivP[22a] and FeTPP[22b] in benzene). Upon addition of greater than 1 M imidazole we observe growth of a band at about 500 cm^{-1}, at the expense of the 521-cm^{-1} band. In the RR spectrum of six-coordinate (6c) Fe^{II}PocPiv(NMeIm)(CO) there are two bands at 500 and 568 cm^{-1}, which show sensitivity to ^{13}CO isotopic substitution (top spectra in Figure 1). The 500-cm^{-1} band, which shifts down to 496 cm^{-1} in the ^{13}CO adduct, is the Fe–C stretching mode, ν_{FeC}. Changing the proximal ligand from NMeIm to 1,2-Me_2Im causes only a slight upshift in the Fe–C stretch, to 502 cm^{-1} (496 cm^{-1} for ^{13}CO—middle two spectra in Figure 1). There is a small residual 5c-CO component (weak 521 cm^{-1}), even though imidazole is present at high (1.2–1.3 M) concentrations.

The 568-cm^{-1} band, present in both the NMeIm and 1,2-Me_2-Im adducts of Fe^{II}COPocPiv (Figure 1), is assigned to the Fe–C–O bending mode, δ_{FeCO}, on the basis of its 8–9-cm^{-1} downshift upon ^{13}CO substitution. This frequency and isotope shift are consistent with those seen in the CO adducts of a number of heme proteins and model compounds,[1] as summarized in Table I. Variability in the reported magnitude of the ^{13}CO downshift of δ_{FeCO} among the entries in Table I probably arises from overlap of the δ_{FeCO} mode with nearby porphyrin modes, which differ among different heme–CO adducts because of their sensitivity to the specific porphyrin peripheral substitution pattern and to interactions with the protein. The C–O stretch, ν_{CO}, of $Fe^{II}\alpha$-PocPiv(NMeIm)(CO) in benzene, has been reported to be 1964 cm^{-1} in the IR spectrum;[8] we were not able to observe the RR band for this mode with 413.1-nm excitation of the adduct in methylene chloride. The ν_{FeC} and δ_{FeCO} modes of Fe^{II}PocPiv-(1,2-Me_2Im)(CO) are the same to within 1 cm^{-1} in methylene chloride and benzene.

2. Capped Porphryin (C_2-Cap). Figure 2 shows the low-frequency (420–660 cm^{-1}, lower spectra) and high-frequency (1925–2025 cm^{-1}, upper spectra) regions of the 413.1-nm excited RR spectra of $Fe^{II}C_2$-Cap(NMeIm)(CO) in benzene, containing 2.6 M NMeIm. As shown in the inset, the benzene cap is attached at positions 1, 2, 4, and 5 to all four of the porphyrin C_m-phenyl substituents by ortho linkers containing an ester, a pair of methylenes, and an ether group. The strong 497-cm^{-1} RR band of $Fe^{II}C_2$-Cap(NMeIm)(CO) is the Fe–C stretching mode, as evidenced by the 4-cm^{-1} downshift of this mode upon ^{13}CO substitution. A weak RR band at 2002 cm^{-1} shifts down 44 cm^{-1} to 1958 cm^{-1} upon ^{13}CO substitution and is the C–O stretch. The frequency is the same as seen in the IR spectrum in toluene.[20c] The ^{13}CO RR spectrum shows an underlying 1996-cm^{-1} band, which is assigned to a porphyrin combination band. The Fe–C–O bending mode is *not* activated in $Fe^{II}C_2$-Cap(NMeIm)(CO); no ^{13}CO sensitivity is observed in the RR bands between 550 and 600 cm^{-1}. The dashed line in Figure 2 marks an isotope-insensitive 568-cm^{-1} band, assigned to a porphyrin mode of C_2-Cap.

The Fe^{II}(NMeIm)(CO) adduct of the four-atom diether-linked capped porphyrin, OCCO,[21] was also examined by RR spectroscopy, with 413.1-nm excitation. This complex in benzene is extremely photolabile. Using less than 1-mW laser power at the sample and a very defocused beam, we were able to obtain at best a mixture of 60% 6c CO-bound and 40% 5c CO-photoproduct, as judged by the high-frequency ν_4 and ν_2 skeletal modes. Under these conditions, we were unable to find a candidate Fe–C stretching band between 400 and 550 cm^{-1}. The CO photolysis was reversible, as the 6c Fe^{II}(NMeIm)(CO) absorption spectrum was recovered following laser irradiation. The enhanced photolysis is attributable to a deceleration of the CO recombination by the steric constraint of the OCCO cap. The CO-binding affinity is also reduced.[21] A very high C–O stretching frequency, 2014 cm^{-1}, has been reported for this adduct from IR spectroscopy.[21]

3. Unconstrained Porphyrins. We were able to observe both the ν_{FeC} and ν_{CO} RR bands of the 6c imidazole–CO adducts of two water-soluble tetraphenylporphyrins in 100 mM phosphate

(20) (a) Hashimoto, T.; Dyer, R. L.; Crossley, M. J.; Baldwin, J. E.; Basolo, F. *J. Am. Chem. Soc.* **1982**, *104*, 2101–2109. (b) Ellis, P. E., Jr.; Linard, J. E.; Szymanski, T.; Jones, R. D.; Budge, J. R.; Basolo, F. *J. Am. Chem. Soc.* **1980**, *102*, 1889–1896. (c) Jones, R. D.; Budge, J. R.; Ellis, P. E., Jr.; Linard, J. E.; Summerville, D. A.; Basolo, F. *J. Organomet. Chem.* **1979**, *181*, 151–158.

(21) Johnson, M. R.; Seok, W. K.; Ibers, J. A. *J. Am. Chem. Soc.* **1991**, *113*, 3998–4000.

Table I. Vibrational Frequencies and Isotope Shifts (cm^{-1}) of the FeCO Linkage in Carbonyl Complexes of Iron Porphyrins and Selected Heme Proteins

no.	molecule/solvent	ν_{FeCO}	$\Delta^{13}C$[a]	$\Delta^{18}O$[a]	ν_{CO}	$\Delta^{13}C$	$\Delta^{18}O$	δ_{FeCO}	$\Delta^{13}C$	$\Delta^{18}O$	ref
1[b]	FeOEP/Bz[c]	531	5	10	1975			n.re.[d]			22b, 83
2	FeTPP/Bz	524	5	{14}[e]	1973[f]						22b, 23
3	FeDeut(THF)/THF	530		{13}	1962		{90}	n.re.			22b
4	FeTSMP(H_2O)/pH 7	527[g]			1957			n.re.			this work
5	FeTPivP(THF)/THF	526	5	10	1957			n.re.			22a,b
6	cyt *c* oxidase	520	4		1964	46		578	14		28a,b
7	FeSP-13(NMeIm)/MC[h]	514	4		1932	44		579	11		16
8	elephant Mb, pH 8.2	515	3	6	1937		{91}	579	16	1	42
9	FeSP-14(NMeIm)/MC[h]	512	4	5	1939	45		578	15	3	16
10	$FePiv_2C_8$(NMeIm)/Bz[i]	515	5		1948	44		576	21		17
11	sperm whale Mb, pH 8.4[j]	512	3	8	1944	48	48	577	14	1	18
12	FeSP-15(NMeIm)/MC[h]	509	6		1945	44		574	11		16
13	sperm whale Mb, pH 7.0	507	3		1947			575	16		64, 60b
14	$FePiv_2C_9$(NMeIm)/Bz[i]	506	5		1948	44		n.re.			17
15	human Hb A[k]	507	4	9	1951	43	43	578	15	2	18
16	$FePiv_2C_{10}$(NMeIm)/Bz[i]	497	3		1952	42		n.re.			17
17	Feα-MedPoc(ImH)/MC	498	4	9	1954[l]	45		567	10	4	38, 8a
18	heme-5(NMeIm)/MC[h]	495	4	9	1954	44					16
19	PPDME(ImH)/MC	495			1960[m]						29
20	Feα-PocPiv(NMeIm)/MC	500	4		1964[n]			568	9		this work, 8a
21	FeTPivP(1,2-Me_2Im)/Bz[o]	496	5		1962						22a,b
22	FeAPC(NMeIm)/Bz[p]	491		{9}	1959			576	{16}		22b, 39
23	$FePiv_2C_{12}$(NMeIm)/Tol	488	4		1958	46		n.re.			17
24	FeOEP(NMeIm)/Bz	496		8	1970						22a, 20a
25	mutant Mb His(E7)Gly, pH 7[q]	492			1965						44a
26	FeTPivP(NMeIm)/Bz	489	4	8	1966–9						22a,b, 8b
27	sperm whale Mb, pH 2.6	489			1966			n.re.			67, 64, 60b
28	FeTPP(1,2-Me_2Im)/Bz	494			1972						22a, 20a
29	Hb M Boston-α^M	490	2	7	1972	48	48				49a
30	FeTSPP(2MeIm)/pH 7	489			1972			n.re.			this work
31	FeTSMP(4MeIm)/pH 7	486	4		1969	39		n.re.			this work
32	FeTPP(py)/Bz	484[r]	4	9	1976	43	43				42
33	FeC_2-Cap(NMeIm)/Bz	497	4		2002[s]	44		n.re.			this work
34	mutant pig Mb His(E7)Val, Val(E11)Thr	479			1984						45a,b
35	cyt P-450$_{CAM}$ from *P. putida* + camphor	481[t]	3	8	1940	43		558	14	3	46a,b
36	FeTPivP($C_6HF_4S^-$)/ClBz	479	5		1956[u]						84a,b
37	cyt P-450$_{CAM}$ from *P. putida* (no substrate)	464–9			1963	45		n.re.			46a,b, 52a
	Feα-PocPiv/MC	521						n.re.			this work
	Feα-PocPiv(1,2-Me_2Im)/MC	502	6					568	8		this work
	Feα-TalPoc(NMeIm)/Bz				1963						8a
	mutant Mb His(E7)Tyr, pH 7	494						n.re.			75b
	mutant human Hb (βE7)Gly[v]	493			1971						44b
	FeTPP(NMeIm)/Bz	486	{11}								22a,b
	FeAnth77(NMeIm)/Cf				1966						39
	FeAnth66(NMeIm)/Cf				1975						39
	FeC_3-Cap(NMeIm)/Tol				1979						20c
	FeOCCO(NMeIm)/Tol				2014						21
	PPDME(Im^-)/MC	490			1942						29
	cyt P-450$_{SCC}$ (no substrate)	477[w]	7		1953	46					46c
	cyt P-450$_{LM}$ (no substrate)	474[x]	5								46e

[a] $\Delta^{13}C$ and $\Delta^{18}O$ are isotope shifts for $^{13}C^{16}O$ and for $^{12}C^{18}O$. [b] Numbered entries are plotted in Figure 3; the remaining entries are not plotted but are relevant to the discussion. [c] Solvent abbreviations: Bz = benzene, THF = tetrahydrofuran, MC = methylene chloride, Tol = toluene, ClBz = chlorobenzene, Cf = chloroform. [d] n.re. indicates not resonance enhanced with excitation near the Soret band. [e] { } indicates frequency shift for the $^{13}C^{18}O$ isotopomer. [f] Measured for crystalline sample. [g] 529 cm^{-1} for FePPIX(H_2O) at pH 9.2.[22b] [h] The solvent was MC for ν_{CO} but 10% MC in Bz for ν_{FeC} and δ_{FeCO}. [i] The solvent was Tol for ν_{CO} but Bz for ν_{FeC} and δ_{FeCO}. [j] ν_{FeC} = 508 cm^{-1} and δ_{FeCO} = 579 cm^{-1} for the Val(E11)Glu mutant.[75b] [k] The same frequencies are seen for the (βE7)Gln and (βE11)Ile mutants.[44b] [l] Obtained in Bz with NMeIm. [m] 1969 cm^{-1} in Bz.[33] [n] Obtained in Bz. [o] ν_{FeC} = 492 cm^{-1}, δ_{FeCO} = n.re., ν_{CO} = 1966 cm^{-1} in MC (this work). [p] The solvent was Cf for ν_{CO} but 10% MC in Bz for ν_{FeC} and δ_{FeCO}. [q] ν_{FeC} = 495 cm^{-1} and ν_{CO} = 1964 cm^{-1} for His(E7)Met mutant. [r] 490 cm^{-1} in MC.[22a] [s] Same frequency in Tol[20c] and 2000 cm^{-1} in Nujol mull.[13] [t] 473 cm^{-1} when norcamphor replaces camphor.[48] [u] Obtained in Bz. [v] Same frequencies for (βE7)Val; ν_{FeC} = 492 cm^{-1} and ν_{CO} = 1968 cm^{-1} for (βE7)Phe. [w] Increases to 478–487 cm^{-1} on binding different cholesterol derivatives.[46d] [x] 473 cm^{-1} for Thr(301)Ser and 476 cm^{-1} for Thr(301)Val mutants.[46f,g]

buffer, pH 7, using 413.1-nm Soret excitation (Table I). The 4MeIm–CO adduct of Fe^{II} tetrakis(*p*-sulfonatomesityl)porphyrin (TSMP) has ν_{FeC} = 486 cm^{-1} and ν_{CO} = 1969 cm^{-1}. These assignments are based on ^{13}CO downshifts of 4 and 39 cm^{-1}, respectively. We also observed the 1969-cm^{-1} C–O stretch of Fe^{II}TSMP(4MeIm)(CO) by FTIR spectroscopy (Nicolet 730), in 0.1-mm path-length anaerobic $CaCl_2$ cells. The 489-cm^{-1} ν_{FeC} and 1972-cm^{-1} ν_{CO} RR bands of the 2MeIm–CO adduct of Fe^{II} tetrakis(*p*-sulfonatophenyl)porphyrin (TSPP) are similar to those of the TSMP adduct. The Fe–C–O bending mode was not observed in either case.

In the absence of added imidazole, the ν_{FeC} and ν_{CO} bands of Fe^{II}TSMP(CO) are at 527 and 1957 cm^{-1}; these are assigned to a 6c CO species with water as a weak sixth ligand, on the basis of their similarity with those of 6c Fe^{II}TPivP(THF)(CO) in THF solution[22] (526 and 1957 cm^{-1}). In the noncoordinating solvent, benzene, the corresponding frequencies for 5c Fe^{II}TPP(CO) are 524 and 1973 cm^{-1}.[22b,23] Dicarbonyl adducts are ruled out since ν_{CO} = 2042 cm^{-1} for $Fe^{II}TPP(CO)_2$.[23]

Discussion

1. Back-Bonding Produces Negative ν_{Fe}/ν_{CO} Correlations. Several workers have noted a negative correlation between the

(22) (a) Kerr, E. A.; Mackin, H. C.; Yu, N.-T. *Biochemistry* **1983**, *22*, 4373–4379. (b) Kerr, E. A. Ph.D. Dissertation, Georgia Institute of Technology, Atlanta, GA, 1984.

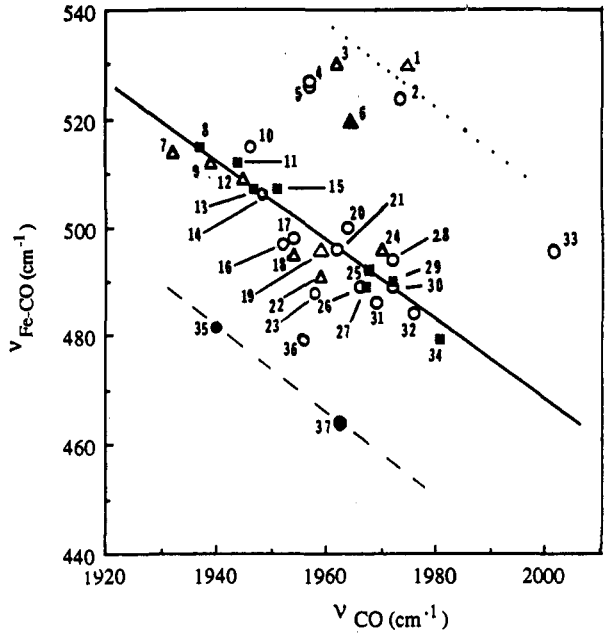

Figure 3. Plot of observed ν_{FeC} vs ν_{CO} frequencies in $Fe^{II}CO$ heme adducts of tetraarylporphyrins (open circles), C_β-alkyl porphyrins (open triangles), globins (solid squares), cytochrome P450s (solid circles), and cytochrome oxidase (solid triangle). The numbers correspond to the entries in Table I. The solid line indicates the backbonding correlation line for proximal neutral imidazoles as given in ref 24. The dashed line is for anionic thiolates, and the dotted line is for five-coordinate CO adducts with no proximal ligand.

ν_{FeC} and ν_{CO} frequencies for a variety of heme–CO adducts and have discussed this effect in terms of back-bonding in the FeCO unit.[1,24-27] The CO ligand is a σ donor and a π acceptor. The d_π electrons of the Fe^{II} ion are donated back to the empty π^* orbitals of CO. This shift in the electron population of the orbitals increases the Fe–C bond order, while decreasing the C–O bond order. As a result, the Fe–C stretching frequency increases while the C–O stretching frequency decreases. Conversely, effects that decrease the extent of back-bonding decrease ν_{FeC} while increasing ν_{CO}.

When ν_{FeC} is plotted against ν_{CO} for CO adducts of a variety of heme proteins having proximal histidine ligands, or for protein-free heme–CO adducts having imidazole or pyridine ligands trans to the CO, then a linear correlation is observed, corresponding to the solid line drawn in Figure 3. The points in Figure 3 represent data from selected heme proteins (filled symbols) to be discussed below and an exhaustive set of data on protein-free complexes (open symbols); the numbering scheme is given in Table I. Those complexes having imidazole ligands fall close to the solid line, which represents a least-squares fit to the larger protein data base considered by Li and Spiro.[24]

Large deviations from this line are observed for complexes with trans ligands that are significantly stronger or weaker donors than imidazole. Stronger donor ligands, such as the imidazolate or thiolate anions, enhance back-bonding from Fe^{II} to CO but at the same time weaken the Fe–C σ bond by competing for the Fe^{II} d_{z^2} orbital.[24] Consequently, the ν_{FeC}/ν_{CO} points fall below the imidazole correlation. When different thiolate-ligated heme–CO adducts (cytochromes P450 and model complexes) are plotted (points 35–37), then a new linear correlation is observed, lying below the imidazole correlation (dashed line in Figure 3), as has been noted by others.[26,27] Additional examples of cyt P450 and peroxidase $Fe^{II}CO$ adducts which fall along the thiolate back-bonding line are given in refs 24 and 27.

Ligands that are weaker donors than imidazole decrease back-bonding but increase the Fe–C σ bond strength, and their ν_{FeC}/ν_{CO} points fall above the imidazole correlation. At constant weak ligation, a higher-lying line is expected. This expectation is illustrated by the dotted line in Figure 3, which is drawn between the points for benzene solutions of the monocarbonyl adducts of FeOEP (point 1) and FeTPP (point 2), in the absence of any sixth ligand. Points falling somewhat below this line belong to CO adducts in weakly coordinating solvents, THF for Fe deuteroporphyrin (point 3) and FeTPivP (point 5) and H_2O for FeTSMP (point 4). Point 6 belongs to the cytochrome a_3 binding site of cytochrome c oxidase. Its position midway between the solid and dotted lines in Figure 3 indicates that the bond from the proximal histidine to the heme Fe is unusually weak, a conclusion supported by the abnormally low Fe-His stretching frequency that has been reported for the CO-free a_3 site of reduced deoxy cytochrome c oxidase.[28a-d]

A similar but less dramatic strengthening of the Fe–C bond is seen when the axial imidazole bond is weakened by proximal steric hindrance. Thus, the 1,2-Me_2Im complex of Fe^{II}TPivP-(CO) (point 21) lies significantly higher in Figure 3 than does the NMeIm complex (point 26), reflecting a stronger Fe–C bond.[22a] Similarly, the 1,2-Me_2Im complex of Fe^{II}TPP (point 28) lies higher than the pyridine complex (point 32). Interestingly, an upshift of only 2 cm^{-1} in ν_{FeC} is seen between the NMeIm and 1,2-Me_2Im complexes of the distally constrained PocPiv adduct (Figure 1). The absence of a larger upshift is surprising, since, in the CO-free complexes, the Fe^{II}–N_{His} stretching frequency does shift strongly, from 227 to 215 cm^{-1}, between NMeIm and 2MeIm (same ligand mass).[8a]

Oldfield and co-workers[3,4] have successfully explained the variations in ^{17}O and ^{13}C NMR chemical shifts of heme–CO adducts with the use of this same model of back-bonding with superimposed σ effects of the axial ligand. Indeed, the ^{17}O shifts correlate very well with ν_{CO}, while the ^{13}C shifts correlate with ν_{FeC}.

2. Back-Bonding Is Influenced by the Polarity of the CO Environment and by the Porphyrin Electronic Structure. When the axial ligand is held constant, the extent of back-bonding is influenced mainly by the polarity of the environment around the bound CO. Positive charges or positively oriented dipoles near the O atom are expected to stabilize the developing negative charge produced by back-bonding. This effect is especially dramatic when there is an actual H-bond to the carbonyl O atom, as is the case of the CO adduct of the low-pH form of horseradish peroxidase (HRP).[26,29] For this adduct, ν_{FeC} is 537 cm^{-1} while ν_{CO} is 1904 cm^{-1}, placing the point much higher on the correlation[24] than any of those shown in Figure 3. Direct evidence for the H-bond comes from a 2.5-cm^{-1} downshift in ν_{CO} when the adduct is prepared in D_2O.[30] The CO adduct of the low-pH form of cytochrome c peroxidase (CCP)[31] falls nearly as high on the line as does HRP. In this case, X-ray crystallography indicates a H-bond to the carbonyl O atom from a bound water molecule, which is in turn polarized by a H-bond from a distal arginine residue.[32]

(23) Wayland, B. B.; Mehne, L. F.; Swartz, J. *J. Am. Chem. Soc.* **1978**, *100*, 2379–2383.
(24) Li, X.-Y.; Spiro, T. G. *J. Am. Chem. Soc.* **1988**, *110*, 6024–6033.
(25) (a) Tsubaki, M.; Ichikawa, Y. *Biochim. Biophys. Acta* **1985**, *827*, 268–274. (b) Paul, J.; Smith, M. L.; Paul, K.-G. *Biochim. Biophys. Acta* **1985**, *832*, 257–264. (c) Tsubaki, M.; Hiwatashi, A.; Ichikawa, Y. *Biochemistry* **1986**, *25*, 3563–3569.
(26) Uno, T.; Nishimura, Y.; Tsuboi, M.; Makino, R.; Iizuka, T.; Ishimura, Y. *J. Biol. Chem.* **1987**, *262*, 4549–4556.
(27) Smulevich, G.; Miller, M.; Kraut, J.; Spiro, T. G. *Biochemistry* **1991**, *30*, 9546–9558.
(28) (a) Argade, P. V.; Ching, Y. C.; Rousseau, D. L. *Science* **1984**, *225*, 329–331. (b) Yoshikawa, S.; Choc, M. G.; O'Toole, T.; Caughey, W. S. *J. Biol. Chem.* **1977**, *252*, 5498–5505. (c) Salmeen, I.; Rimai, L.; Babcock, G. T. *Biochemistry* **1978**, *17*, 800–806. (d) Ogura, T.; Hon-nami, K.; Oshima, T.; Yoshikawa, S.; Kitagawa, T. *J. Am. Chem. Soc.* **1983**, *105*, 7781–7783. (e) Woodruff, W. H.; Einarsdottir, O.; Dyer, R. B.; Bagley, K. A.; Palmer, G.; Atherton, S. J.; Goldbeck, R. A.; Dawes, T. D.; Kliger, D. S. *Proc. Natl. Acad. Sci. U.S.A.* **1991**, *88*, 2588–2592.
(29) Evangelista-Kirkup, R.; Smulevich, G.; Spiro, T. G. *Biochemistry* **1986**, *25*, 4420–4425.
(30) Smith, M. L.; Ohlsson, P.-I.; Paul, K.-G. *FEBS Lett.* **1983**, *163*, 303–305.
(31) Smulevich, G.; Evangelista-Kirkup, R.; English, A.; Spiro, T. G. *Biochemistry* **1986**, *25*, 4426–4430.

In protein-free adducts, the solvent polarity is expected to play a role. Upshifts along the correlation line (more back-bonding) are indeed observed when adducts are compared for solutions in benzene and the more polar methylene chloride. For Fe^{II}TPP(py), ν_{FeC} shifts up 6 cm^{-1},[22a] while in Fe^{II}PPDME(ImH) ν_{CO} shifts down 9 cm^{-1} between benzene and methylene chloride.[33] When the same comparison is made for Fe^{II}TPivP(py),[22a] however, the ν_{FeC} upshift is only 1 cm^{-1}, indicating that the pivaloyl pickets of the picket fence porphyrin shield the bound CO from the solvent and impose their own polarity via the pivaloylamino groups. All four amide dipoles in the Fe^{II}CO adduct of Fe^{II}TPivP(NMeIm) point toward the center of the molecule.[34] The enhanced polarity is evident from the fact that this adduct in benzene (point 26) is much higher on the correlation line than is Fe^{II}TPP(py) (point 32).

We had expected to see strong polar interactions with water. However, aqueous Fe^{II}TSPP(2MeIm) and Fe^{II}TSMP(4MeIm) (points 30 and 31) actually fall slightly below Fe^{II}TPivP(NMeIm) (point 26) but above Fe^{II}TPP(py) (point 32) in the back-bonding correlation. Thus, the aqueous polarity seems to be less pronounced than that of the picket-fence amide groups. We speculate that the water dipoles are prevented from polarizing the bound CO more effectively because of the orienting effect of the four peripheral negative charges on the sulfonatophenyl substituents.

Back-bonding is also influenced by variations in the electron-donating tendency of the substituents on the porphyrin ring. Thus complexes based on substituted tetraaryl porphyrins (open circles in Figure 3) are generally found lower on the back-bonding correlation than adducts based on C_β-alkyl-substituted porphyrins (open triangles). The alkyl substituents are electron donating and enhance back-donation, while the phenyl substituents are electron withdrawing and decrease back-donation. Because of the dominant role of environmental polarity, however, there is overlap between these two classes of porphyrins. The unconstrained adducts Fe^{II}OEP(NMeIm) (point 24) and Fe^{II}TPP(py) (point 32) in benzene are the representatives of the two classes that lie lowest on the back-bonding correlation.

3. Polarization Can Be Enhanced by Distal Steric Constraint. Tsubaki et al.[18] first reported that ν_{FeC} was elevated in MbCO relative to protein-free heme complexes. It was also observed that ν_{FeC} increased with decreasing strap length in a series of Fe^{II}(NMeIm)(CO) porphyrin complexes having polymethylene chains covalently strapped across a C_β-substituted porphyrin ring.[16] Since the diffraction data for MbCO had been interpreted in terms of a distinctly off-axis geometry for the FeCO,[10,11] Yu and co-workers[16,18] inferred that the cross-porphyrin strap inhibits upright binding of CO, increasingly so as the strap length shortens. They concluded that bending or tilting of the FeCO unit increases the ν_{FeC} frequency. Figure 3 shows that the complexes studied by Yu et al.[16] exhibit increasing back-bonding with decreasing strap length. The complex with the strap having only 13 atoms (point 7) falls highest on the ν_{FeC}/ν_{CO} correlation, followed successively by the complexes with 14- and 15-atom straps (points 9 and 12) and then by the complex with no strap (point 18).[35] A similar progression down the line is seen in another series of polymethylene-strapped porphyrins, the two-picket "basket handle porphyrins" studied by Desbois et al.;[17] points 10, 14, 16, and 23 are for complexes in this series having eight through twelve methylene groups in the strap. Increased back-bonding is again observed when the TPivP complex (point 26) is capped by a benzene ring via single methylene links to the amides, in the PocPiv adduct (point 20) of the present study.

In all these cases, an increase in distal steric constraint correlates with an increase in back-bonding. Yet this trend is not easily understood as a consequence of FeCO geometric distortion. As discussed by Li and Spiro,[24] FeCO bending should strongly *decrease* back-bonding. The electronic effects of FeCO tilting and porphyrin ruffling are more difficult to predict, but an increase in back-bonding is not an obvious outcome.

The present data on C_2-Cap demonstrate dramatically that distal constraint does *not* necessarily increase back-bonding. The CO adduct of this porphyrin (point 33), in which a benzene cap is attached via ester and ether links to TPP, has a much higher ν_{CO} frequency, 2002 cm^{-1}, than does any other adduct in Figure 3. The only report of a higher ν_{CO} frequency (2014 cm^{-1}) is for another benzene-capped porphyrin, OCCO, which has even shorter links to TPP, again based on ether bonds.[21] As mentioned above, we were unable to obtain the RR spectrum of this adduct, because it is photolabile.

Why does a benzene cap produce such different ν_{CO} frequencies for PocPiv and for C_2-Cap? The answer cannot lie in FeCO geometry differences. As seen in Table II, the FeCO unit is only slightly off axis and to about the same extent in the two cases. The C_2-Cap crystals[13] have two independent molecules in the unit cell, with Fe–C–O angles of 176 and 173° and Fe–C tilt angles of 4 and 6°, respectively; the perpendicular displacement of the O atom from the porphyrin normal through the Fe atom is 0.3 and 0.4 Å, respectively. For the PocPiv adduct,[12] the corresponding parameters are 173°, 6°, and 0.4 Å, respectively. These structural parameters are for the 1,2-Me_2Im adduct of the β atropisomer of PocPiv,[12] but little structural difference is expected for the NMeIm adduct of the α-atropisomer (point 20), since the CO binding affinities of their Fe^{II}(1,2-Me_2Im) adducts are the same for the two atropisomers[12] and since ν_{FeC} is within 2 cm^{-1} for the NMeIm and 1,2-Me_2Im adducts (Figure 1). It is apparent that FeCO angular distortion does not control the vibrational frequencies in these sterically constrained porphyrin adducts and that electronic effects must do so.

These electronic differences undoubtedly result from the nature of the linkages from the porphyrin to the benzene cap. PocPiv has amide links, with the N-H dipoles turned inward, providing an environment of positive polarity for the CO ligand. As mentioned above, this amide polarity effect accounts for TPivP (point 26) being higher on the back-bonding correlation than TPP (point 32) and being insensitive to the nature of the solvent. The fact that PocPiv (point 20) is even higher on the correlation can be attributed to the bound CO being pushed closer toward one of the amide NH groups by the steric constraint of the cap. Indeed the crystal structure shows that the O atom of the bound CO is 3.8 Å from one of the amide N atoms in PocPiv[12] versus 4.9 Å in TPivP[36] (Table II). The same effect can account for the back-bonding trends seen for the strapped porphyrins studied by Yu et al.[16] and for the basket handle porphyrins studied by Desbois et al.[17] (who recognized the importance of H-bonding for the kinetics of O_2 binding of their complexes). For both series of compounds, the polymethylene straps are linked to the porphyrins via *amide* bonds. The NH groups provide positive polarity in the vicinity of the bound CO, and the polar interaction can be increased via the steric constraint of short straps. This effect can readily explain the fact that back-bonding increases with decreasing strap length in both series of compounds.[37] [For the basket handle porphyrin with the longest (12 methylene groups) handle, Piv_2C_{12}, the FeCO unit is known[36b] to be linear, and the N(H)···O distance

(32) Edwards, S. L.; Poulos, T. L. *J. Biol. Chem.* **1990**, *265*, 2588–2595.

(33) Caughey, W. S. In *Methods for Determining Metal Ion Environments in Proteins: Structure & Function of Metalloproteins*; Darnall, D. W., Wilkins, R. G., Eds.; Elsevier North-Holland: New York, 1980; pp 95–115.

(34) Collman, J. P.; Gagne, R. R.; Halbert, T. R.; Hoard, J. L.; Reed, C. A.; Sayler, A. A. Unpublished crystal structure of Fe(II)TPivP(NMeIm)(CO). Quoted by: Hoard, J. L. In *Porphyrins and Metalloporphyrins*; Smith, K. M., Ed.; Elsevier: Amsterdam, 1975; Chapter 8, p 358.

(35) We note that solvents of different polarity were used to obtain the Fe–C (RR in 10% CH_2Cl_2 in benzene) and C–O (IR in neat CH_2Cl_2) stretching frequencies of these porphyrins.[16] Solvent effects on the FeCO frequencies are expected to be significant for the unconstrained heme-5 reference compound; an estimated 6–9-cm^{-1} upshift in the ν_{CO} frequency in going from CH_2Cl_2 to benzene, based on the reported organic solvent effects on ν_{CO},[33] would move the heme-5 (point 18) closer to the correlation line.

(36) (a) Estimated[34] from the analogous untethered-picket distances in the crystal structure of $Fe^{II}Piv_2C_{12}$(NMeIm)(CO);[36b] see footnote *h* in Table II. (b) Ricard, L.; Weiss, R.; Momenteau, M. *J. Chem. Soc., Chem. Commun.* **1986**, 818–820.

Table II. Structural Parameters for the Indicated $Fe^{II}(X)(CO)$ Porphyrin Complexes[a]

	TPP (py)	Deut (THF)	Piv_2C_{12} (NMeIm)	β-PocPiv (1,2-Me_2Im)	C_2-Cap (NMeIm)
r_{Fe-C}, Å	1.77	1.706	1.728	1.768	1.742, 1.748[b]
C_{disp}, Å[c]	0.04	0.07	0.0	0.18	0.17, 0.12
O_{disp}, Å[c]	0.08	0.15	0.0	0.38	0.41, 0.28
σ_{bend}, deg	179	178.3	180.0	172.5	172.9, 175.9
ϕ_{tilt}, deg[d]	1.4	2.5	0.0	6.2	5.6, 3.9
r_{Cap-Fe}, Å[e]			8.43	5.36	5.57, 5.68
r_{Cap-O}, Å[f]			5.56	3.99	2.77, 2.80
r_{Am-O}, Å[g]			4.60[h]	3.76[i]	
conf[j]	pln	roof	dom	ruf	sad, sad
ref	82	85	36b	12	13

[a] Obtained from the referenced structural papers or calculated[86a] from porphyrin coordinates deposited in the Cambridge data base.[86b] Estimated standard deviation in the distances is ca. 0.01 Å and in the angles is ca. 1 deg. [b] Values for the two independent molecules/unit cell.[13] [c] X_{disp} is the perpendicular displacement from the heme normal for the indicated atom. [d] ϕ_{tilt} is the angle between the Fe–C bond and the heme normal. [e] r_{Cap-Fe} is the distance between the centroid of distal cap or strap and Fe atom; it defines the distal pocket size. [f] r_{Cap-O} is the distance between the centroid of the distal cap or strap and the carbonyl O; it is a measure of Cap-CO steric contact. [g] r_{Am-O} is the shortest distance between amide-N on the cap linker arms and the carbonyl O. [h] 4.60 Å for amides in the strap vs 4.87 Å for amides in the pickets. [i] Distances are 3.76, 6.33, and 4.55 Å for three inequivalent cap linker arms of PocPiv. [j] Porphyrin conformations: pln = planar, roof = roof fold along line joining opposite C_m atoms, dom = domed, ruf = ruffled (S_4), sad = saddled (S_4).

for the amides in the strap is long, 4.6 Å (Table II). Corresponding structure parameters are unavailable for other members of this series or for the strapped porphyrins.] Increased back-bonding is also observed in the pocket porphyrin series as the strap length is shortened (Table I); ν_{CO} shifts down from 1969 cm^{-1} in TPivP to 1963 cm^{-1} in the tall pocket porphyrin (TalPoc, three methylene links)[8] to 1954 cm^{-1} in the medium pocket porphyrin (MedPoc, two methylene links),[8] while ν_{FeC} shifts up from 489 to 498 cm^{-1}.[38]

In C_2-Cap, there are no NH groups to provide positive polarity near the CO ligand. The lone pairs of the ester groups provide negative polarity. So does the π electron cloud of the benzene cap, which is very close to the carbonyl O atom; the center of the benzene ring is only 2.77 and 2.80 Å away, for the two independent molecules in the cell.[13] This short-range interaction with the π cloud is expected to inhibit back-donation from the Fe^{II} d_π to the CO π* orbitals and can account for the unusually high ν_{CO} at 2002 cm^{-1}. No doubt the same effect produces the even higher frequency in the OCCO adduct, 2014 cm^{-1}. In the C_2-Cap adduct, the benzene ring moves 1.7 Å away from the porphyrin to accommodate CO binding inside the cavity,[13] a motion that is restricted by the shorter cap-linker arms in the OCCO adduct. When the linker arms are extended by one methylene group, in C_3-Cap, the CO frequency decreases to 1979 cm^{-1},[20c] owing to attenuation of the benzene cap interaction.[20a] A smaller effect in the same direction, 1975 to 1966 cm^{-1}, is seen when the linker arms are extended between 6,6- and 7,7-anthracene cyclophane porphyrins.[39]

In the PocPiv adduct, the distance from the carbonyl O atom to the center of the benzene cap is 3.99 Å, 1.2 Å further than in C_2-Cap, because, in the former, the cap slips to one side of the CO. Sideways slippage is prevented for C_2-Cap and OCCO because the benzene ring is anchored by four links to the four porphyrin phenyl substituents, while one of these links is missing in PocPiv. Some interaction with the benzene ring in PocPiv can, nevertheless, be inferred from the fact that ν_{CO} *decreases* from 1964 to 1954 cm^{-1} upon extending the linker arms by one methylene group in MedPoc porphyrin.[8] The MedPoc adduct lies higher on the back-bonding correlation in Figure 3 (point 17) than does PocPiv (point 20), indicating that in the former the interaction with the amide group is maintained while the interaction with the cap is attenuated.

While the π cloud interaction explains the high C–O stretching frequency, it is also significant that the C_2-Cap adduct (point 33) falls well above the back-bonding correlation in Figure 3. The Fe–C frequency is 30 cm^{-1} higher than expected for such a high C–O frequency, on the basis of the back-bonding correlation.[40] This elevation cannot be due to a weak axial ligand, since ligation by NMeIm was definitely established in our titration experiments (see Experimental Section) and the Fe–N(imidazole) bond is normal (2.04 Å) in the crystal structure.[13] Instead, we ascribe the rise in ν_{FeC} to compression of the Fe–C bond in C_2-Cap, caused by the short contact of the carbonyl ligand with the benzene ring. The reduction in back-bonding produced by this contact should lengthen the Fe–C bond, because of the reciprocal relationship between C–O and Fe–C bond orders. But this lengthening is prevented by the cap. From Badger's rule we estimate the Fe–C bond compression in C_2-Cap to be 0.05 Å, using the 30-cm^{-1} ν_{FeC} elevation from the back-bonding correlation.[41] Thus, part of the steric constraint of the benzene cap is accommodated by compressing the Fe–C bond. We note that the Fe–C distance in the two C_2-Cap molecules is 1.74 and 1.75 Å (Table II), while it is 1.77 Å in PocPiv, even though a shorter Fe–C bond is expected in the latter because of its enhanced back-bonding. The esd's of ca. 0.01 Å, however, limit the significance of this comparison.

A small amount of Fe–C bond compression can also be inferred for PocPiv relative to MedPoc. Despite the 10-cm^{-1} increase in ν_{CO} between MedPoc and PocPiv, the expected decrease in ν_{FeC} is not observed; instead, ν_{FeC} shifts up 2 cm^{-1}. Thus, the cap in PocPiv, though farther from the carbonyl than in C_2-Cap (Table II), shows the same tendency to decrease back-bonding while compressing the Fe–C bond but to a much smaller extent. The ν_{FeC} elevation from the back-bonding line is only 6 cm^{-1} in the PocPiv adduct, corresponding to a bond compression of 0.01 Å, on the basis of Badger's rule.

4. Pocket Polarity Also Determines FeCO Frequencies in Heme Proteins. Although the FeCO geometry was an initial focus for RR analysis of heme protein CO adducts, it is becoming clear that the polarity of the bound CO environment is the main determinant of the Fe–C and C–O frequencies in the proteins as well as in the models. MbCO from elephant[42] lies significantly higher on the back-bonding correlation (point 8) than do MbCO from sperm whale (point 13) and human HbCO (point 15), although the distal histidine of the latter two is replaced in the former by a smaller side chain from glutamine, which might have been expected to allow a more upright FeCO geometry.[43] But

(37) We note that two ν_{FeC} bands of similar intensities were reported for the shortest strap adducts in both these series and were attributed to variable strap–CO interactions.[16,17] We believe that the lower frequency bands, ca. 500 cm^{-1}, are attributable to a bis-CO adduct; the Fe–C stretches of bis-CO adducts of heme-5 and OEP formed at high CO pressures in benzene are reported[22b] at 498–500 cm^{-1}. The imidazole concentration was low (0.5–100 mM) in the RR experiments.[16,17] In our experience, a larger excess of imidazole (1–2 M) is needed to prevent CO from binding on the unhindered side of constrained porphyrins. The higher frequency bands[16,17] are assumed to represent the mono-CO, monoimidazole adducts and were used in constructing Figure 3.

(38) Mitchell, M. L. Ph.D. Dissertation, Princeton University, Princeton, NJ, 1984.

(39) (a) Traylor, T. G.; Tsuchiya, S.; Campbell, D.; Mitchell, M.; Stynes, D.; Koga, N. *J. Am. Chem. Soc.* **1985**, *107*, 604–614. (b) Traylor, T. G.; Mitchell, M. J.; Tsuchiya, S.; Campbell, D. H.; Stynes, D. V.; Koga, N. *J. Am. Chem. Soc.* **1981**, *103*, 5234–5236.

(40) The equation for the back-bonding correlation line of neutral imidazole–CO adducts ν_{FeC} (cm^{-1}) = 1935.3 – 0.7335ν_{CO} (based on the data set in ref 24) yields an expected Fe–C stretching frequency of 467 cm^{-1}, when the C–O stretch is at 2002 cm^{-1}.

(41) (a) Badger's rule[41b] gives $r_e = 0.85 + 1.5k^{-1/3}$, where r_e is the bond distance and k is the force constant, using the Herschbach and Laurie parameters[41c] for Fe–C bonds. The force constant is estimated from the observed (497 cm^{-1}) and expected (467 cm^{-1}) frequencies using the diatomic harmonic oscillator approximation:[41d,e] $\nu(cm^{-1}) = 1303.1[F(\mu_x + \mu_y)]^{1/2}$. (b) Badger, R. M. *J. Chem. Phys.* **1935**, *3*, 710–714. (c) Herschbach, D. R.; Laurie, V. W. *J. Chem. Phys.* **1961**, *35*, 458–463. (d) Spiro, T. G.; Czernuszewicz, R. S.; Li, X.-Y. *Coord. Chem. Rev.* **1990**, *100*, 541–571. (e) Herzberg, G. *Molecular Spectra and Molecular Structure: II. Infrared and Raman Spectra of Polyatomic Molecules*; Van Nostrand Reinhold: New York, 1945; p 173.

(42) Kerr, E. A.; Yu, N.-T.; Bartnicki, D. E.; Mizukami, H. *J. Biol. Chem.* **1985**, *260*, 8360–8365.

when the distal histidine is replaced by nonpolar residues, e.g., glycine, valine, or phenylalanine, in site-directed mutants of either Mb[44a] or Hb,[44b] then ν_{FeC} falls to 491–493 cm^{-1} and ν_{CO} rises to 1965–1971 cm^{-1}; there is little variation in these frequencies despite the large differences in the size of the side chains (Table I). The data for Mb His(E7)Gly are representative, and its point (25) in Figure 3 shows very weak back-bonding. We infer that MbCO and HbCO show greater back-bonding than the mutants with nonpolar distal E7 residues because the distal histidine, or glutamine for elephant Mb, provides a positive polar interaction[44b] for the bound CO. As noted above, the CO adducts of HRP and CCP in their low-pH forms show still greater back-bonding, owing to a H-bond formed with distal residues.

Further support for the dominance of pocket polarity effects comes from the recent observation that the His(E7)Val, Val(E11)Thr double mutant of pig Mb [H64V-V68T] gives rise to an abnormally high ν_{CO}, 1984 cm^{-1},[45a,d] and an abnormally low ν_{FeC}, 479 cm^{-1}.[45b] It falls on the back-bonding correlation at a point (34) lower than observed for any other heme protein CO adduct. In particular, it is lower than the points characteristic of CO in a nonpolar environment, implying that back-bonding is inhibited by the double mutation. The reason for this can be seen in the crystal structure[45a] of the single mutant, Val(E11)Thr of pig Mb [V68T]. The Val 68 side-chain is adjacent to the bound CO, and the Thr OH group might have been expected to add positive polarity to the environment. Indeed, replacement of Val 68 with asparagine in human Mb[45c] has been found to shift ν_{CO} down to 1915 cm^{-1}. However, the Thr 68 OH group donates a H-bond to a backbone carbonyl group, and therefore the O atom lone pairs are oriented toward the bound CO, providing a source of *negative* polarity. In the absence of the positively polar distal histidine E7, this interaction inhibits backbonding in the double mutant. The effect is akin to the benzene cap interaction in C_2-Cap, although no deviation from the back-bonding line, indicative of Fe–C bond compression, is seen for the protein.

It is instructive to examine the data for cytochrome P450 from the point of view of back-bonding changes. Although only data for cyt $P450_{CAM}$ are plotted in Figure 3 (points 37 and 35), it has been observed for a number of P450 enzymes that substrate binding increases ν_{FeC} and decreases ν_{CO}, shifting the data points upward along the back-bonding correlation[46] (Table I). The cyt P450 heme pocket is mostly nonpolar,[47a] but the crystal structure of the CO adduct of camphor-bound cyt $P450_{CAM}$ shows that the steric bulk of the camphor displaces the O atom of the CO toward a polar groove of the pocket.[47b] This groove contains the side chain of the Thr 252 residue, whose OH group forms a H-bond to the backbone carbonyl of Gly 248. Thr 252 is highly conserved in P450 enzymes and is believed to play an essential role in proton transfer to the terminal O atom of bound O_2 in the P450 monooxygenase mechanism.[47a] The structural data strongly suggest that camphor binding increases FeCO back-bonding in the CO adduct by forcing the CO into a more polar environment, in a manner entirely analogous to the sterically constrained porphyrins with amide side groups, as discussed above. (We note that replacement of the conserved distal Thr by Ser or Val in microsomal $P450_{LM}$ has very little (±3 cm^{-1}) effect on the Fe–C stretching frequency.[46f] But the crystal structure of the Thr(252)Ala mutant of $P450_{CAM}$ with bound camphor[47c] reveals that a solvent molecule not present in the native enzyme is positioned in the distal groove. Thus a solvent molecule may provide a polar contact with bound CO in the Thr(252) mutants.)

5. RR Intensity Is Enhanced for δ_{FeCO} but Diminished for ν_{FeC} by Polar Interactions. Tsuboi has proposed[48] that the ^{13}C-sensitive band at 560–580 cm^{-1} is actually the *overtone* of the bending mode rather than its fundamental. This proposal allowed Tsuboi to interpret the frequency upshift in ν_{FeC} upon substrate binding to cyt P450(CO) as resulting from substrate-induced bending of the FeCO unit. As discussed by Li and Spiro,[24] FeCO bending produces a strong interaction between ν_{FeC} and δ_{FeCO}, and their frequencies spread apart. Since the former is near 500 cm^{-1}, its frequency decreases with FeCO bending, provided δ_{FeCO} is at 560–580 cm^{-1}. But if the δ_{FeCO} fundamental is instead at 280–290 cm^{-1}, then ν_{FeC} would increase upon FeC bending. Using Tsuboi's proposal, Nagai et al.[49a] similarly explained the decrease in ν_{FeC} in Hb mutants having tyrosine substitutions for the distal histidine (Hb M Boston, point 29) as resulting from relief of FeCO bending in native HbCO. As discussed in the preceding section, however, both the cyt P450 alterations upon substrate binding, and the effects of distal histidine replacement by other residues in Mb or Hb, are adequately explained in terms of interactions with polar groups in the heme pocket, without any involvement of FeCO bending. Since the idea that the vibrational frequencies detect bending in native HbCO continues to be advanced,[49b] it is important to settle the issue of the bending mode frequency. In Appendix 1, we present arguments to establish that the ca. 560-cm^{-1} band *is* the FeCO bending fundamental, as originally assigned,[18] and not its overtone.

The FeCO bending mode is seen in the RR spectra of many heme proteins and in sterically constrained porphyrins but not in porphyrins lacking steric constraints. This behavior led Yu et al. to conclude that the bending mode enhancement is an indicator of off-axis CO binding.[16] We observe this mode for PocPiv (Figure 1) but *not* for C_2-Cap (Figure 2), even though the off-axis displacement is essentially the same for both CO adducts (Table II). Thus, the FeCO geometry cannot be the determinant of δ_{FeCO} activation.

As pointed out earlier,[24] the bending mode ordinarily lacks a mechanism for enhancement in the RR spectrum. If the heme–CO adduct retains effective 4-fold symmetry, then the FeCO bending mode is of E symmetry. Such a mode cannot be enhanced via the A term (Franck–Condon) mechanism, which applies only to totally symmetric modes, nor the B term (vibronic) mechanism, which, in porphyrins, applies to modes of A_2, B_1, and B_2 symmetry that mix the in-plane π–π^* electronic transitions.[50] Consequently, if the FeCO bending mode *is* enhanced, then the 4-fold symmetry must be lost. In that case the bending mode acquires totally symmetric character, and Franck–Condon activation is available to the extent that the degree of bending changes in the resonant excited state.

(43) (a) Likewise, the Hb A Val(E11)Ile mutant[44a] is as high on the backbonding correlation as Hb A (Table I), even though the crystal structure of the former[43b] shows that the extra δ-methyl group of the larger Ile residue imposes additional steric hindrance on the FeCO unit and blocks the ligand binding site. (b) Nagai, K.; Luisi, B.; Shih, D.; Miyazaki, G.; Imai, K.; Poyart, C.; De Young, A.; Kwiatkowsky, L.; Noble, R. W.; Lin, S.-H.; Yu, N.-T. *Nature* **1987**, *329*, 858–860.

(44) (a) Morikis, D.; Champion, P. M.; Springer, B. A.; Sligar, S. G. *Biochemistry* **1989**, *28*, 4791–4800. (b) Lin, S.-H.; Yu, N.-T.; Tame, J.; Shih, D.; Renaud, J.-P.; Pagnier, J.; Nagai, K. *Biochemistry* **1990**, *29*, 5562–5566.

(45) (a) Cameron, A. D.; Smerdon, S. J.; Wilkinson, A. J.; Habash, J.; Helliwell, J. R.; Li, T.; Olson, J. S. Submitted for publication. (b) Biram, D.; Garratt, C. J.; Hester, R. E. In *Spectroscopy of Biological Molecules*; Hester, R. E., Girling, R. B., Eds.; Royal Society of Chemistry: Cambridge, U.K., 1991; pp 433–434. (c) Balasubramanian, S.; Lambright, D. G.; Marden, M. C.; Boxer, S. G. *Biochemistry* **1993**, *32*, 2202–2212. (d) Li, T.; Quillin, M. L.; Phillips, G. N., Jr.; Olson, J. S. submitted for publication in *Biochemistry*.

(46) (a) Uno, T.; Nishimura, Y.; Makino, R.; Iizuka, T.; Ishimura, Y.; Tsuboi, M. *J. Biol. Chem.* **1985**, *260*, 2023–2026. (b) O'Keefe, D. H.; Ebel, R. E.; Peterson, J. A.; Maxwell, J. C.; Caughey, W. S. *Biochemistry* **1978**, *17*, 5845–5852. (c) Makino, R.; Iizuka, T.; Ichikawa, Y. *Proceedings of the IXth International Conference on Raman Spectroscopy*; Tokyo, Japan, Aug 27-Sept 1, 1984; p 492. (d) Tsubaki, M.; Hiwatashi, A.; Ichikawa, Y. *Biochemistry* **1987**, *26*, 4535–4540. (e) Anzenbacher, P.; Evangelista-Kirkup, R.; Schenkman, J.; Spiro, T. G. *Inorg. Chem.* **1989**, *28*, 4491–4495. (f) Egawa, T.; Imai, Y.; Ogura, T.; Kitagawa, T. *Biochim. Biophys. Acta* **1990**, *1040*, 211–216. (g) Ozaki, Y.; Kitagawa, T.; Kyogoku, Y.; Imai, Y.; Hashimoto-Yutsudo, C.; Sato, R. *Biochemistry* **1978**, *17*, 5826–5831.

(47) (a) Poulos, T. L.; Finzel, B. C.; Howard, A. J. *J. Mol. Biol.* **1987**, *195*, 687–700. (b) Raag, R.; Poulos, T. L. *Biochemistry* **1989**, *28*, 7586–7592. (c) Raag, R.; Martinis, S. A.; Sligar, S. G.; Poulos, T. L. *Biochemistry* **1991**, *30*, 11420–11429.

(48) Tsuboi, M. *Ind. J. Pure Appl. Phys.* **1988**, *26*, 188–191.

(49) (a) Nagai, M.; Yoshimasa, Y.; Kitagawa, T. *Biochemistry* **1991**, *30*, 6495–6503. (b) Lian, T.; Locke, B.; Kitagawa, T.; Nagai, M.; Hochstrasser, R. M. *Biochemistry* **1993**, *32*, 5809–5814.

(50) Spiro, T. G.; Czernuszewicz, R. S. In *Physical Methods in Bioinorganic Chemistry*; Que, L., Ed.; University Science Books: Mill Valley, CA, in press.

This symmetry lowering can, of course, be effected by pushing the CO off-axis. But the symmetry can also be lowered by off-axis charges or dipoles that polarize the FeCO bonds. The latter mechanism must be operative in PocPiv, since the slight off-axis distortion is insufficient in itself to activate δ_{FeCO}, as demonstrated by C_2-Cap. The amide group near the CO ligand in PocPiv provides the needed off-axis dipole, which is missing in C_2-Cap. When symmetrically disposed, as in TPivP, the amide groups do *not* activate δ_{FeCO}.[51] The asymmetric interaction forced by the steric constraint is required for activation.

The bending mode is also seen in all three methylene strapped porphyrins (points 12, 9, 7)[16] and in adamantane strapped hemin (APC, point 22).[22b,39] As the chain length is shortened in the strapped hemes, there is an increase in intensity of the FeCO bend relative to the FeC stretch.[16] Tightening the constraint probably forces stronger asymmetric polar interactions with one of the linking amide groups, simultaneously increasing back-bonding and δ_{FeCO} enhancement.

In heme proteins as well, the evidence favors an electrostatic mechanism for δ_{FeCO} enhancement. The mode is observed for both MbCO and HbCO[18] even though only a slight off-axis displacement of the CO has been determined crystallographically for the latter.[15] It is *not* seen for mutants having a hydrophobic replacement for the distal histidine, regardless of the size of the side chain.[44a,b] It is strongly enhanced for the low-pH forms of HRP[26,29] and CCP,[31] in which the bound CO is H-bonded to a distal residue, but it disappears for the high-pH forms, which lack such an interaction.[27] In fact, the appearance of δ_{FeCO} in proteins correlates well with the extent of back-bonding. Species with significant back-bonding, at the level of neutral-pH MbCO or higher, show the bend, while others which are low on the back-bonding correlation do not. Among globins high on the back-bonding correlation, the intensity ratio of the FeCO bend relative to the FeC stretch increases in parallel with upshifts in their positions along the line.[16,42] Distal polar interactions in heme proteins will destroy the 4-fold symmetry of the heme, except in the unlikely event that the interaction is directed exactly along the heme normal.

For cyt P450 adducts, δ_{FeCO} is enhanced for substrate-bound forms,[46a] consistent with the postulated substrate enforcement of a polar groove interaction with the CO, but is extremely weak for the substrate-free form.[52a,b] A point of some interest is that the CO adduct of cytochrome *c* oxidase shows δ_{FeCO} activation,[28a] implying a distal polar interaction in this case as well. Although a protein side chain may provide this interaction, another possibility is that the Cu^+ ion of the binuclear site is responsible. The CO has been found to bind to the Cu^+ ion within 1 ps of photodissociation from the heme Fe, implying a short transit path.[28e]

Examination of Figures 1 and 2 reveals that the intensity of the Fe–C stretching RR band also differs significantly between PocPiv and C_2-Cap, under conditions of minimal (<5%) CO photolysis (as monitored by the ν_4 and ν_2 skeletal modes). The integrated intensity is three times higher in C_2-Cap than in PocPiv, using the porphyrin 447- and 635-cm^{-1} bands as internal standards. A survey of published spectra suggests that the Fe–C band intensity correlates negatively with back-bonding. When there are polar interactions that increase back-bonding, the RR intensity of ν_{FeC} seems to be systematically lower than when such interactions are absent. In part, this phenomenon results from intensity borrowing by δ_{FeCO}. When the bending mode is activated, then the excited state is displaced along the Fe–C stretching and Fe–C–O bending coordinates simultaneously, and the two modes share the overall intensity resulting from the change in orbital occupation. In addition, the ν_{FeC} intensity may be lower because of a smaller excited-state displacement. The Fe–C bond length is altered in the π–π^* excited state of the porphyrin because the porphyrin and CO π^* orbitals compete for the Fe d_π electrons. Occupation of the porphyrin π^* orbitals in the excited state diminishes back-bonding to the porphyrin and enhances back-bonding to the CO. Since enhancement of ν_{FeC} increases with the extent of excited-state displacement along the Fe–C stretching coordinate, the intensity depends on the *difference* in FeCO back-bonding between the ground and excited states. When back-bonding in the ground state is enhanced, the change in back-bonding upon electronic excitation is expected to diminish.

Table III. FeCO Distortion and Binding Energies (kcal/mol)

		PocPiv		C_2-Cap	
distortion coord[a]	k[b]	q[c]	V[d]	q	V
σ(FeCO)	0.80 mdyn-Å	7.5°	0.99	5.6°	0.55
ϕ(FeCO)	0.72 mdyn-Å	6.2°	0.61	4.8°	0.36
Δd(FeC)	2.5 mdyn/Å	0.01 Å	0.02	0.05 Å	0.45
$2\sum V_i$[e]			3.2		2.7
$\Delta\Delta G$[f]			2.5		3.3
$\delta(2\sum V_i - \Delta\Delta G)$			+0.7		–0.6

[a] Key:

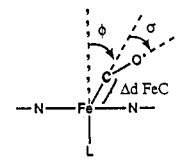

[b] Vibrational force constant. [c] Magnitude of distortion. [d] Distortion energy: $V_i = {}^1/_2 k_i q_i^2$. [e] Estimate of the total steric energy (see text). [f] Binding free energy change (affinity decrease): $\Delta\Delta G = \Delta G_{CO}^{ref} - \Delta G_{CO}$ relative to the reference compound $Piv_3$5CIm. $\Delta G_{CO} = -RT \ln K$ for FeP(L) + CO = FeP(L)(CO).

6. Energetics of FeCO Binding and Distortion. The structural and vibrational data on the PocPiv and C_2-Cap adducts permit estimation of the energetics of FeCO distortion. For small displacements of the atoms from their equilibrium positions, the required energies can be estimated from the harmonic approximation, $V = (kq^2)/2$, where q is the change in an internal coordinate (bond stretching or bending) and k is the associated force constant. The relevant internal coordinate changes are the deviation of the FeCO angle from linearity, σ (bending angle), the deviation of the Fe–C bond direction from the heme normal, ϕ (tilt angle), and the Fe–C bond compression, Δd (see Table III). The force constants have been estimated by Li and Spiro[24] to be 0.80 mdyn-Å, 0.72 mdyn-Å, and 2.5 mdyn/Å, respectively. Table III lists the energies stored in these distortion coordinates for the PocPiv and C_2-Cap adducts. The bend and tilt angles are taken from the crystal structures,[12,13] while the bond compression is estimated from the deviation of the Fe–C stretching frequency from the value expected on the basis of the back-bonding correlation, as discussed above.

The energies involved are small, as expected, since the displacements are small. For C_2-Cap, the three distortion coordinates each store about 0.5 kcal/mol, for a total of 1.4 kcal/mol. On the other hand, bond compression contributes negligible energy in PocPiv, because the Fe–C bond is already shortened by the enhanced back-bonding from the distal polar interaction, as discussed above. The angle distortions are somewhat larger in PocPiv and store a total of 1.6 kcal/mol. In both adducts, bending and tilting store similar amounts of energy. The actual displacement of the CO ligand is, however, more effectively accommodated by tilting than by bending. Each degree of tilting produces a much larger off-axis displacement of the O atom than does bending, because the Fe···O distance is almost three times as long as the C–O distance. In the PocPiv adduct, for example, the 6.2° tilt is responsible for 0.3 Å, out of the total 0.4 Å, O atom displacement from the heme normal.

(51) In our RR spectrum of Fe^{II}TPivP(1,2-Me_2Im)(CO) with low (<5%) CO photolysis, ν_{FeC} is seen strongly at 492 cm^{-1} (relative to the 447- and 635-cm^{-1} porphyrin bands), but δ_{FeCO} is not observed.

(52) (a) Champion, P. M. In *Biological Applications of Raman Spectroscopy, Vol. 3: Resonance Raman Spectra of Heme and Metalloproteins*; Spiro, T. G., Ed.; Wiley-Interscience: New York, 1988; pp 249–292. (b) Although an Fe–C–O bend has been reported for substrate-free cyt $P450_{CAM}$, no ^{13}C-sensitive band can be seen in the published spectra.[46a]

These energetic estimates refer only to the distortions produced by steric crowding and leave out of account additional electronic factors, such as the distal interaction of the bound CO with the amide NH groups in the PocPiv adduct or with the benzene π cloud plus the ester lone pairs in the C_2-Cap adduct. The former interaction should be stabilizing, while the latter should be destabilizing.

These electronic energies can be gauged by comparing the steric energies with the total interaction energies, as determined from CO affinity changes relative to a suitable unconstrained reference compound. In toluene, the CO binding constants[7] are (in units of M^{-1}) $10^{7.83}$ and $10^{7.28}$ for the NMeIm complexes of PocPiv and C_2-Cap but $10^{9.66}$ for Piv_35CIm,[7] a porphyrin with three pivaloylamino "pickets" and an internally coordinated imidazole ligand attached as a covalent "tail".[53] The diminished binding constants for the constrained porphyrins translate to binding free energy changes of 2.5 and 3.3 kcal/mol for PocPiv and C_2-Cap, respectively. These energies should reflect both steric and electronic differences between the two adducts. (In addition they contain solvation energy differences between bound and unbound complexes, but these differences are expected to be similar in the two cases.) To estimate the total steric energy, we double the energy stored in the three FeCO distortion coordinates, because the force required to produce these distortions must be applied by the porphyrin and its superstructure, which must therefore store energy in distortions of the covalent framework.[54a] The energy stored in these framework distortions is unknown but is probably similar in magnitude to the energy stored in the FeCO distortions. The entries in Table III show that this estimate of the total steric energy exceeds the binding free energy change by 0.7 kcal/mol for PocPiv but falls short by 0.6 kcal/mol for C_2-Cap. These deviations are in the direction expected for stabilizing and destabilizing electronic interactions in the two adducts, respectively, and therefore lend credence to the steric energy estimates.

What is surprising is how small these electronic energies seem to be. The affinity reductions of the constrained porphyrins mainly result from the steric interactions. The difference in the estimated electronic energies between PocPiv and C_2-Cap is only 1.3 kcal/mol, even though the one has NH groups and the other has a benzene ring and ester lone pairs close to the bound CO. Yet it is the electronic interactions that produce the back-bonding changes that mainly determine the vibrational frequencies, as the above discussion makes clear. We conclude that the vibrational frequencies are quite sensitive to electronic influences on the highly polarizable FeCO unit, even though these influences do not produce large interaction energies. The heme-bound CO is a sensitive probe of the heme environment.

From this analysis we infer that large distortions of the FeCO unit are precluded simply by the prohibitive cost in CO binding energy. Since electronic energies associated with distal interactions are not large, the binding energy decreases more or less in proportion to the steric energy. Rather than adopt a severely distorted structure, CO will simply not bind, except at very high pressures of CO. An interesting test of this picture would be provided by the crystal structure of the CO adduct of the severely constrained porphyrin, OCCO.[21] The half-saturation CO pressure for its NMeIm complex in toluene is very high, 100 Torr, $10^{6,7}$-fold higher than for Piv_35CIm,[7] corresponding to a 9.1 kcal/mol binding energy loss. Assuming that this is close to twice the distortion energy, and that the latter is divided equally among bending, tilting, and bond compression, as is approximately true for C_2-Cap, then the predicted bending and tilting angles would be 9.4 and 9.9°. It seems unlikely that distortions much larger than this can be induced by steric constraints.

Opportunities for distortion would seem to be even more limited in proteins, since the conformational mobility of the polypeptide make large steric energies unlikely. Crystal structures of Fe^{II}-CO adducts of several heme proteins indicate that CO binding is accommodated by displacements of distal groups and the heme.[54b] It has recently been determined, via site-directed mutagenesis, that replacing the distal histidine in sperm whale Mb with glycine increases the CO affinity by 1.0 kcal/mol.[55] This replacement should relieve steric hindrance by the imidazole side chain and also reduce the polarity of the heme pocket. The latter effect is indeed apparent from the downshift along the back-bonding correlation (Figure 3), but the associated electronic energy is suggested from the model compound data to be small. This inference is supported by the recent finding by Li et al.[45d] that for a series of Mb mutants the logarithm of the CO dissociation rate constant correlates with ν_{CO}, consistent with its expected dependence on the Fe–C bond strength, and therefore on electronic factors, but the slope of the correlation is only 0.02 log units per cm^{-1}. Since the His(E7)Gly mutation shifts ν_{CO} from 1947 to 1965 cm^{-1}, this correlation predicts a loss in electronic stabilization energy of 0.5 kcal. Li et al. find no correlation with ν_{CO} of either the CO association rate constant or the binding equilibrium constant, both of which show a much larger range of variation than does the dissociation rate constant. This behavior is completely consistent with our conclusion that steric effects can inhibit CO binding without significant influence on the FeCO geometry or vibrational frequencies. If we assume that relief of steric inhibition accounts for the 1 kcal/mol affinity increase in His(E7)Gly, in the face of a 0.5 kcal/mol electronic destabilization, then a total steric energy of 1.5 kcal/mol is implied for native Mb. If half of this is stored in the protein and half in the FeCO distortion, then the expected CO displacement is small, ca. 5° each of bending and tilting.

This energy estimate may actually be too large, however, in view of evidence[45a] that water binding to the distal imidazole in deoxy Mb may inhibit CO binding. A water molecule within H-bond distance of His E7 is seen in deoxy Mb crystals,[14] and in the Val(E11)Thr mutant this water molecule is further anchored by H-bonding to the Thr OH lone pair.[45a] This stabilization of the water molecule accounts for the 5-fold decrease in CO affinity associated with the Val(E11)Thr mutation. Cameron et. al.[45a] suggest that the bound H_2O in wild-type Mb may explain the affinity increase when His E7 is replaced by Gly.

We note that steric and electronic effects on the binding energetics are very different for CO and O_2, as Traylor[6,9] and others[20a,54c,55,56] have emphasized. While both CO and O_2 draw electrons from Fe^{2+} upon binding to deoxyheme, the extent of electron transfer is much greater for O_2, which develops significant negative charge.[1,57] Interactions with distal polar groups are larger for O_2, as reflected in much larger changes in binding affinity. These differential effects on CO and O_2 affinity have been well documented in model compounds[9,7,20a,56] and proteins.[54c,55] In the case of the Mb His(E7)Gly mutant, for example, the O_2 affinity *decreases* by 1.6 kcal/mole, owing to the decrease

(53) This reference compound was chosen because of its internal imidazole ligand. In contrast to the sterically constrained porphyrins, unconstrained porphyrins bind two exogenous imidazole ligands, rather than only one, complicating the interpretation of CO binding data. This problem can be circumvented by comparing CO adducts with sterically hindered imidazoles, but as noted above, the sterically hindered imidazole may be accommodated differently by encumbered and unencumbered porphyrins.

(54) (a) In PocPiv,[12] the benzene cap shifts 3.3 Å off-center away from the bound CO, while in C_2-Cap,[13] the cap moves 1.7 Å further away from the porphyrin ring to accommodate CO binding inside the cavity. (b) In MbCO the distal His N_ϵ and Val $C_{\gamma 1}$ atoms move, respectively, by 1.7 and 0.5 Å away from the bound CO relative to deoxy Mb, and the heme group slides 0.24 Å further into the heme pocket.[11] In HbCO[15] significant porphyrin deformation (buckling) and greater (~1.0 Å) movement of the heme absorbs some of the steric strain.[54c] In CCP(CO),[32] and $P450_{CAM}(CO)$,[47b] distal groups move away from bound CO relative to the ferric protein, by 0.6 Å (Arg-48) and by 0.8 Å (distal camphor), respectively. (c) Perutz, M. F. *Trends Biochem. Sci.* **1989**, *14*, 42–44.

(55) Olson, J. S.; Mathews, A. J.; Rohlfs, R. J.; Springer, B. A.; Egeberg, K. D.; Sligar, S. G.; Tame, J.; Renaud, J.-P.; Nagai, K. *Nature* **1988**, *336*, 265–266.

(56) Ward, B.; Wang, C.-B.; Chang, C. K. *J. Am. Chem. Soc.* **1981**, *103*, 5236–5238.

(57) Jameson, G. B.; Drago, R. S. *J. Am. Chem. Soc.* **1985**, *107*, 3017–3020.

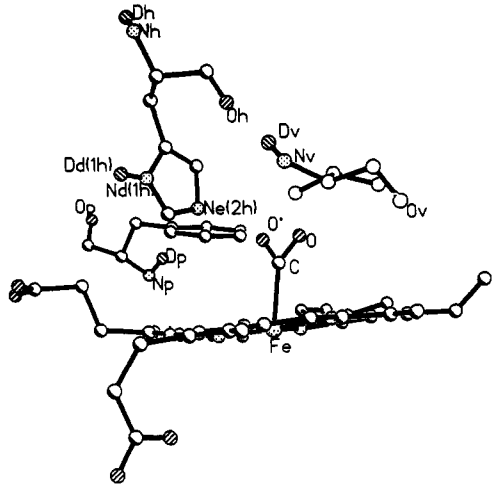

Figure 4. Disposition of the heme–CO in the MbCO neutron structure[10] and the distal residues His E7 (H64 = h), Phe CD1 (F43 = p), and Val E11 (V68 = v). The placement of deuterium atoms is shown. The CO oxygen atom is disordered, with O and O′ indicating its half-occupancy positions.

in pocket polarity, while the CO affinity increases.[55] An additional manifestation of the CO/O_2 difference is the H-bond donated from the distal histidine to the bound O_2 in MbO_2,[58] which is not present in MbCO.[10c,d]

7. MbCO and Its Substates. We turn to the puzzle posed by the crystal structures of sperm whale MbCO.[10,11] How can the protein induce significant off-axis distortion, as has been claimed, when the electronic preference for perpendicular binding is so large? The preceding analysis suggests that the protein does not generate steric forces large enough to do so. Consistent with this view, a very recent X-ray structure of sperm whale MbCO expressed in *E. coli* from a synthetic gene, and crystallized in a form having ordered CO, shows only a slight deviation from perpendicular binding (σ(FeCO) = 169°),[14] as does the X-ray structure of HbCO (σ(FeCO) = 173°).[15] Similarly small deviations are observed for mutant MbCO's in which the distal histidine is replaced by Gly, Leu, or Gln.[14] Also, NMR analysis has established a ligand tilt of ca. 15° for the cyanide adduct of metMb, as well as its His(E7)Val mutant;[59] the $Fe^{III}CN^-$ unit should be easier to bend than $Fe^{II}CO$ since there is less back-bonding in the former. It is likely that the much larger deviations from linearity reported for the earlier MbCO crystal structures, in which the CO was disordered, are not experimentally significant. This question is addressed in Appendix 2.

A more serious issue is that the neutron structure analysis[10] finds no proton on N_ϵ, the distal histidine nitrogen atom that is adjacent to the bound CO; apparently the imidazole proton resides instead on N_δ, where it is stabilized by interaction with a water molecule.[10] This means that a lone pair, rather than a H-bond donor, faces the bound CO, as illustrated in Figure 4. Yet, as discussed above, MbCO falls midway up the back-bonding correlation (Figure 3), implying a significantly positive polar interaction.

A possible resolution of this dilemma may lie in the existence of multiple substates of MbCO. The IR spectrum of MbCO contains several, overlapping ν_{CO} bands.[60,61a] The frequency used in Figure 3, 1947 cm^{-1}, is the main component in solution.[60b] This band is broad and asymmetric and has been fit to two components, a major one at 1946 and a minor one at 1941 cm^{-1} by Frauenfelder and co-workers[61a,62] (although Caughey and co-workers[60c,d,e] have fit the band to a major component at 1944 and a minor component at 1952 cm^{-1}). Two other IR bands are also observed, at 1966 and 1932 cm^{-1}. Their intensities, relative to the main band, vary with temperature,[60d,62b,63] with pressure,[62c] with solution conditions (pH and ionic strength),[44a,60b,d,64] and among crystals prepared in different ways.[60c] These four ν_{CO} IR components have been studied extensively by Frauenfelder and co-workers,[61a,62,65] who attribute them to different conformational substates of the protein, labeled A_0–A_3, in order of decreasing frequency. The substates exhibit different kinetic parameters for CO photodissociation and recombination,[61a] and they have different inclinations of the CO ligand relative to the heme normal, as determined by IR photoselection experiments.[65,66] We tentatively suggest a structural scheme for these substates, as shown in Figure 5, based on the following considerations.

The A_0 substate results from protonation of the distal imidazole.[44a,64,67,68] When the pH of MbCO solutions is lowered, the 1966-cm^{-1} ν_{CO} band increases in intensity in concert with a 490-cm^{-1} ν_{FeC} band.[44a,60b,64] This pair of frequencies lies low on the backbonding correlation (point 27) and is typical for nonpolar environments, as exmplified by mutant MbCO with nonpolar replacements of the distal histidine;[44a] a ν_{CO} band of 1969 cm^{-1} is also observed for Fe^{II}PPDME(ImH) in benzene.[33] The pK_a of the transition is ca. 4.4 [64] and is within experimental error of the pK_a determined via NMR spectroscopy[69] for the distal histidine. This low pK_a is attributed to the nonpolar environment of the heme pocket. Protonation requires that the His E7 residue swing out of the heme pocket and extend into the solution, as has recently been established via the low-pH crystal structure of MbCO.[70] (Other perturbations than pH may also remove the histidine from the vicinity of the CO. For example, dehydration of HbCO has been observed to enhance the A_0 population.[71]) Champion and co-workers[44a,68] have studied this transition in detail and have determined microscopic pK_a's of 3.8 and 6.0 for protonation of the imidazole in the "closed" and "open" forms, respectively.[44a] They have also shown[68] that the transition occurs in MbCO crystals that are bathed in solutions of varying pH and that the 490-cm^{-1} A_0 band is very weak at pH values higher than 6. Likewise, the IR spectrum reported by Makinen et al.[60c] of MbCO crystals at neutral pH shows little or no intensity at 1967 cm^{-1}. Thus the A_0 substate is not significantly populated near

(58) (a) Phillips, S. E. V.; Schoenborn, B. P. *Nature (London)* **1981**, *292*, 81–82. (b) Phillips, S. E. V. *J. Mol. Biol.* **1980**, *142*, 531–554.

(59) Rajarathnam, K.; Qin, J.; La Mar, G.; Chiu, M. L.; Sligar, S. G. *Biochemistry* **1993**, *32*, 5670–5680.

(60) (a) McCoy, S.; Caughey, W. S. In *Probes of Structure and Function of Macromolecules and Membranes, Vol II*; Chance, B., Yonetani, T., Mildvan, A. S., Eds.; Academic Press: New York, 1971; pp 289–293. (b) Fuchsman, W. H.; Appleby, C. A. *Biochemistry* **1979**, *18*, 1309–1321. (c) Makinen, M. W.; Houtchens, R. A.; Caughey, W. S. *Proc. Natl. Acad. Sci. U.S.A.* **1979**, *76*, 6042–6046. (d) Caughey, W. S.; Shimada, H.; Choc, M. G.; Tucker, M. P. *Proc. Natl. Acad. Sci. U.S.A.* **1981**, *78*, 2903–2907. (e) Potter, W. T.; Hazzard, J. H.; Choc, M. G.; Tucker, M. P.; Caughey, W. S. *Biochemistry* **1990**, *29*, 6283–6295.

(61) (a) Ansari, A.; Berendzen, J.; Braunstein, D.; Cowen, B. R.; Frauenfelder, H.; Hong, M. K.; Iben, I. E. T.; Johnson, J. B.; Ormos, P.; Sauke, T. B.; Scholl, R.; Schulte, A.; Steinbach, P. J.; Vittitow, J.; Young, R. D. *Biophys. Chem.* **1987**, *26*, 337–355. (b) Mourant, J. R.; Braunstein, D. P.; Chu, K.; Frauenfelder, H.; Nienhaus, G. U.; Ormos, P.; Young, R. D. Submitted for publication in *Biophys. J.*

(62) (a) Frauenfelder, H.; Sligar, S. G.; Wolynes, P. G. *Science* **1991**, *254*, 1598–1603. (b) Hong, M. K.; Braunstein, D.; Cowen, B. R.; Frauenfelder, H.; Iben, I. E. T.; Mourant, J. R.; Ormos, P.; Scholl, R.; Schulte, A.; Steinbach, P. J.; Xie, A. H.; Young, R. D. *Biophys. J.* **1990**, *58*, 429–436. (c) Frauenfelder, H.; Alberding, N. A.; Ansari, A.; Braunstein, D.; Cowen, B. R.; Hong, M. K.; Iben, I. E. T.; Johnson, J. B.; Luck, S.; Marden, M. C.; Mourant, J. R.; Ormos, P.; Reinisch, L.; Scholl, R.; Schulte, A.; Shyamsunder, E.; Sorensen, L. B.; Steinbach, P. J.; Xie, A. H.; Young, R. D.; Yue, K. T. *J. Phys. Chem.* **1990**, *94*, 1024–1037.

(63) Berendzen, J.; Braunstein, D. *Proc. Natl. Acad. Sci. U.S.A.* **1990**, *87*, 1–5.

(64) Ramsden, J.; Spiro, T. G. *Biochemistry* **1989**, *28*, 3125–3128.

(65) Ormos, P.; Braunstein, D.; Frauenfelder, H.; Hong, M. K.; Lin, S.-L.; Sauke, T. B.; Young, R. D. *Proc. Natl. Acad. Sci. U.S.A.* **1988**, *85*, 8492–8496.

(66) Moore, J. N.; Hansen, P. A.; Hochstrasser, R. M. *Proc. Natl. Acad. Sci. U.S.A.* **1988**, *85*, 5062–5066.

(67) Han, S.; Rousseau, D. L.; Giacometti, G.; Brunori, M. *Proc. Natl. Acad. Sci. U.S.A.* **1990**, *87*, 205–209.

(68) Zhu, L.; Sage, J. T.; Rigos, A. A.; Morikis, D.; Champion, P. M. *J. Mol. Biol.* **1992**, *224*, 207–215.

(69) Wilbur, D. J.; Allerhand, A. *J. Biol. Chem.* **1977**, *252*, 4968–4975.

(70) Quillin, M. L.; Brantley, R. E., Jr.; Johnson, K. A.; Olson, J. S.; Phillips, G. N., Jr. *Biophys. J.* **1992**, *61*, A466.

(71) Brown, W. E., III; Sutcliffe, J. W.; Pulsinelli, P. D. *Biochemistry* **1983**, *22*, 2914–2923.

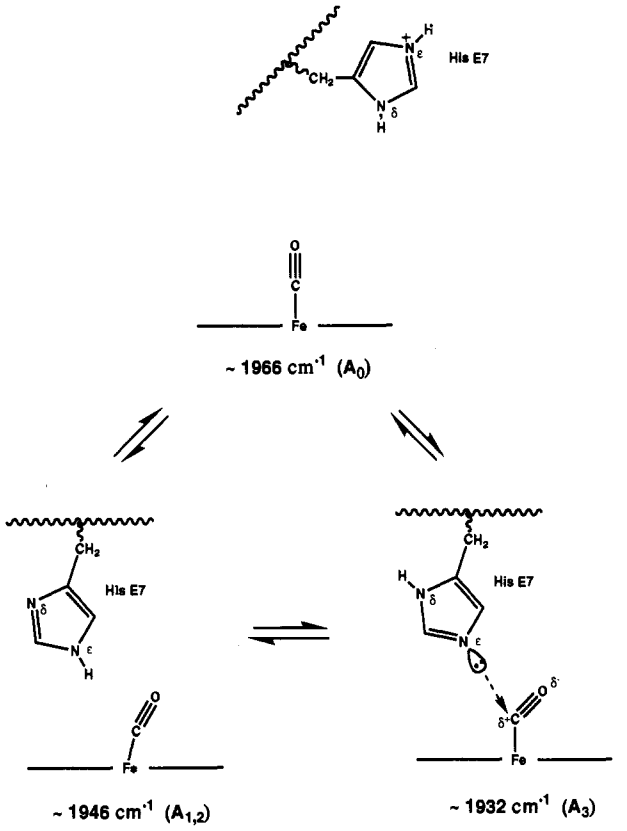

Figure 5. Proposed interactions in the MbCO substates. In A_0 the distal histidine is protonated, and displaced from the heme pocket, leaving the bound CO in a nonpolar environment. The distal histidine (neutral) is in the pocket in the $A_{1,2}$ and A_3 substates and is close to the bound CO. Its tautomeric state has the proton on N_δ in A_3, and the lone-pair on N_ϵ interacts with the CO π^* orbital, inducing some FeCO bending. The $A_{1,2}$ substates have the proton on N_ϵ, lending positive polarity to the CO environment.

neutrality and is not a significant contributor to the X-ray[10] or neutron[11] crystal structures, which were determined at pH values above 5.7.

The A_3 substate, however, is a major contributor to crystalline MbCO. The crystal IR spectrum of Makinen et al.[60c] shows nearly equal intensities for bands at 1933 and 1944 cm^{-1}, whereas the $A_3/A_{1,2}$ IR intensity ratio is lower in solution. Mourant et al.[61b] have recently observed nearly 90% of the population as A_3 in an orthorhombic crystal sample at low temperature. Thus, the A_3 population is specifically enhanced upon crystallization. We propose that $A_{1,2}$ and A_3 are associated with the two alternative tautomers of the distal imidazole, with the proton on N_ϵ and N_δ, respectively. (A_1 and A_2 are very similar and presumably arise from slightly different structures, both associated with the N_ϵ tautomer. A possibility is that they are ring-flip isomers. Oldfield et al.[5] have pointed out that rotation by 180° about the ring–C_β bond leaves the imidazole side chain occupying the same space but with its N atoms in different orientations. Different orientations of the $N_\epsilon H$ group relative to the CO could produce slightly different vibrational frequencies.[72]) The A_3 substate may be favored in crystals because the outer edge of the imidazole is exposed to solvent, and the water molecule to which the N_δ is H-bonded[10a,b] may be stabilized by further H-bonding to sulfate ions in the crystallizing medium. It is possible that the crystal used for the neutron diffraction study[10] contained mainly A_3.

In this scheme, the $A_{1,2}$ vibrational frequencies, which fall midway up the back-bonding correlation, result from a positive polar interaction with the adjacent $N_\epsilon H$ group (Figure 5). The depressed A_3 IR frequency, 1933 cm^{-1}, is then a possible consequence of a weak interaction of the N_ϵ lone pair with the CO π^* orbital, an interaction originally suggested by Caughey and co-workers.[60c,73] Such a donor–acceptor interaction would cause the carbon to acquire some sp^2 character, thereby lowering both ν_{CO} *and* ν_{FeC}. Also RR enhancement should be lowered by the loss in back-bonding. It is therefore significant that no RR band attributable to Fe–C stretching has been clearly identified for A_3. If the A_3 substate obeyed the back-bonding correlation in Figure 3, then ν_{FeC} should occur at ca. 520 cm^{-1}. Recognizing this, Morikis et al.[44a] assigned a 520-cm^{-1} shoulder, detectable in the low-temperature RR spectrum of MbCO, to the A_3 substate. This band is very weak, however, with an intrinsic intensity, estimated on the basis of the IR-determined A_3 population,[44a] to be ca. 10-fold smaller than that of the dominant $A_{1,2}$ band at 508 cm^{-1}. The isotope sensitivity of the 520-cm^{-1} band was not tested, and so an alternative assignment to a porphyrin mode is possible. Thus it is apparent that ν_{FeC} for A_3 is much weaker than for $A_{1,2}$ and/or falls at a lower than expected frequency, consistent with a possible donor interaction from the N_ϵ lone pair.

By inducing some sp^2 character at the carbonyl C atom, such an interaction would also induce FeCO bending. Consistent with this expectation, the IR photoselection experiments indicate a larger angle between the CO vector and the heme normal for A_3 than for $A_{1,2}$. Ormos et al.,[65] using CW photoselection on frozen samples, and Moore et al.,[66] using picosecond photoselection in solution, both obtained 35° for A_3 but smaller values for $A_{1,2}$, 20° in solution[66] and 28° in frozen samples.[65] The meaning of these numbers is not completely transparent, since angles near 20° have been obtained even for a protoheme–CO adduct in aqueous/alcoholic solutions, where perpendicular binding might have been expected on average.[74] Nevertheless, it does appear that the FeCO unit is displaced further from the heme normal in A_3 than in $A_{1,2}$. We emphasize, however, that the CO stretching frequency itself places a severe limit on how much the FeCO unit bends. The A_3 frequency is 1933 cm^{-1}, some 30 cm^{-1} lower than expected for a hydrophobic binding pocket (e.g. A_0), whereas the reduction should have been ca. 200 cm^{-1} if the angle were as small as 120°, a value implying pure sp^2 hybridization, since the expected frequency for sp^2 carbonyls is in the 1700–1800-cm^{-1} region. Thus 120–140° FeCO angles are not plausible even for the A_3 substate (see Appendix 2).

We note that this proposed lone pair interaction is different from that operating in the His(E7)Val, Val(E11)Thr double Mb mutant,[45a] described in section 4, which inhibits back-bonding. The difference must lie in the detailed geometry of the interaction. If the lone pair points at the negative end of the bound CO dipole, i.e. the O atom, then inhibition of back-bonding is expected, whereas, if it points at the positive end, i.e. the C atom, then a donor interaction is possible. The resolution of the protein crystal structures is insufficient to evaluate the interaction geometry at this level of detail.

This account of the multiplicity of distal histidine interactions with the bound CO is supported by the results of site-directed mutagenesis.[43b,44a,55,75] When His E7 is replaced by Gly or Met in Mb, the CO adduct shows dominant ν_{CO} and ν_{FeC} bands at the A_0 positions (ν_{CO} = 1965 cm^{-1}, ν_{FeC} = 492 cm^{-1}),[44a] as expected

(72) Oldfield, et al.[5] proposed that the two ring-flip isomers combined with the two tautomers could account for the four observed substates. They gave a simple three-parameter equation, representing the effect of the imidazole dipole on the CO stretching frequency, and were able to fit the four observed frequencies for sperm whale Mb, and for a range of other heme proteins, to good accuracy. The physical significance of these parameters is uncertain, however, since they appear to run counter to back-bonding expectations. Thus, the highest CO frequency (A_0) was always associated[5] with a near-parallel allignment of the imidazole dipole (with *positive* end pointed at the CO) and the CO bond vector, whereas this orientation would be expected to maximize back-bonding and decrease the CO frequency.

(73) Maxwell, J. C.; Caughey, W. S. *Biochemistry* **1976**, *15*, 388–396.
(74) Hansen, P. A.; Moore, J. N.; Hochstrasser, R. M. *Chem. Phys.* **1989**, *131*, 49–62.
(75) (a) Phillips, G. N., Jr.; Arduini, R. M.; Springer, B. A.; Sligar, S. G. *Proteins: Struct., Funct., Genet.* **1990**, *7*, 358–365. (b) Egeberg, K. D.; Springer, B. A.; Martinis, S. A.; Sligar, S. G.; Morikis, D.; Champion, P. M. *Biochemistry* **1990**, *29*, 9783–9791.

from the nonpolar character of the His E7 replacements. Minor bands are also seen at the A_1 positions (ν_{CO} = 1944 cm^{-1}, ν_{FeC} = 506 cm^{-1}) indicating an additional substate with a polar interaction. The relative amplitudes of the major and minor components are not altered by lowering the pH, however, consistent with the absence of a titratable group in the heme pocket. It seems likely that the minor substate results from interaction of the bound CO with a water molecule that invades the heme pocket part of the time. Partial access to water would result from a loosening of the packing in the heme pocket of the mutant proteins, and indeed a nearby water molecule is resolved in the X-ray structure of the His(E7)Gly mutant of MbCO.[14] (Such an interaction also finds precedent in the structure of the cyt $P450_{CAM}$ mutant Thr(252)Ala,[47c] discussed above, in which a water molecule replaces the Thr 252 OH group next to the bound CO.) No 1933-cm^{-1} band is seen in the His E7 mutant Mb spectra, consistent with the absence of a specific imidazole interaction.

Conclusions

The vibrational data on FeCO adducts of PocPiv and C_2-Cap establish unequivocally that distal polar interactions, rather than FeCO geometric distortions, are the primary determinants of the FeCO vibrational frequencies and of the RR enhancement pattern, in sterically constrained porphyrins. Positive polar interactions increase ν_{FeC} and decrease ν_{CO} along a back-bonding correlation that is monotonic for constant proximal ligation (e.g. imidazole or thiolate); they also activate δ_{FeCO} in the RR spectrum, provided the FeCO axial symmetry is lowered. Steric constraints can, however, enforce polar interactions, and this combination of effects can explain all of the available data on sterically constrained porphyrins. The heme protein data can also be explained on the basis of distal polar interactions, or their absence, using the same back-bonding correlation. The single exception is the MbCO A_3 substate, whose FeC stretching RR band is anomalously weak and/or of low frequency, possibly reflecting a donor interaction from the distal histidine, when its tautomeric state has the proton on N_δ, the tautomer seen in the neutron crystal structure. The vibrational frequencies of the dominant solution substate, $A_{1,2}$, imply a significant positive polar interaction, requiring the proton to be on N_ϵ.

The FeCO group can accommodate steric forces with small amounts of tilting and bending, up to ca. 10° each. The steric forces that would be required for substantially larger angular distortions are too large to be supported by proteins, or by synthetic porphyrin superstructures, and if they could be generated, they would simply inhibit CO binding. Conversely, steric energies can modulate the CO binding energy significantly, even if the angular distortions are small. For MbCO, somewhat greater bending may be present in the A_3 substate, induced by the suggested donor interaction, but even here the CO stretching frequency precludes an FeCO angle small enough to induce significant sp^2 hybridization. Earlier reports of 120–140° angles probably reflect experimental uncertainties in the crystallography (Appendix 2).

Despite the sensitivity of the FeCO vibrational frequencies to polar influences, the electronic interaction energies are small and do not contribute importantly to the binding energies. These interactions are much more important for O_2 binding, because of the greater charge transfer from Fe^{II} to O_2. Thus the CO ligand is a sensitive probe for polar effects that modulate the binding and activation of O_2 rather than of CO itself.

Acknowledgment. We thank Drs. A. J. Wilkinson and J. S. Olson for communicating results prior to publication, Dr. Martin R. Johnson and Mr. M. Cyr for assistance with the samples, and Dr. Doug Ho for assistance in analyzing porphyrin crystal structures in the Cambridge Data base. We have benefited from very useful discussions with Drs. J. M. Guss, G. N. Phillips, Jr., and P. M. Champion. This work was supported by NIH Grant GM 33576 (to T.G.S.). X.-Y.L. acknowledges partial support by an RGC grant (HKUST 10/91) administered by UPGA, Hong Kong.

Table IV. Metal Carbonyl Vibrational Frequencies (cm^{-1}) and Assignments for the MCO Unit

compd (pt group)	orientation[a]	ν(Fe–C) (sym)[b]	δ(Fe–C–O) (sym)	ν(C–O) (sym)	ref
$Fe(CO)_5$ (D_{3h})	ax	415 (A1′)	642 (E′)	2027 (A1′)	77
	eq	446 (A1′)	615 (E′)	2120 (A1′)	
$Cr(CO)_6$ (O_h)		381 (A1g)	665 (F1u)	2112 (A1g)	78
$Mn(CO)_5Br$	ax	473 (A1)	546 (E)	1992 (A1)	79
(C_{4v})	eq	384 (A1)	647 (A1, A2)	2137 (A1)	

[a] ax = axial; eq = equatorial. [b] The frequency is given for the indicated mode symmetry.

Appendix 1: The ca. 560-cm^{-1} Band Is Not the Overtone of FeCO Bending

Tsuboi's overtone proposal[48] rested on his assessment that the 0.8 mdyn-Å FeCO bending force constant required to calculate δ_{FeCO} at ca. 570 cm^{-1} [24] was physically unreasonable. If the fundamental is at half this frequency instead, then the force constant is only 0.2 mdyn-Å. In support of this lower value, Tsuboi cited a force constant of 0.48 mdyn-Å for F–C–O bending in F_2CO, a molecule which he suggested should be more resistant to bending than the FeCO unit. Shimanouchi's original paper on the F_2CO normal mode analysis,[76] however, gave 0.48 *mdyn/Å* as the force constant; conversion to mdyn-Å units requires multiplication by the product of the bond distances, which raises the value to 0.75 mdyn-Å. Moreover, Shimanouchi's Urey–Bradley force field had a large nonbonded force constant between the F and O atoms; it is well-known that such a force constant between the terminal atoms of a bond angle reduces the calculated value of the bending force constant. We estimate that transforming the F–C–O force constant from Shimanouchi's Urey–Bradley force field to a valence force field would raise the value to 1.1 mdyn-Å. In this light the 0.8 mdyn-Å value implied by a FeCO bending fundamental assignment of the ca. 560-cm^{-1} band of FeCO adducts does not seem excessive.

In any event, a more appropriate comparison for the FeCO unit is provided by metal carbonyl complexes, for which extensive vibrational analyses are available (Raman and IR spectra of isotopes and normal coordinate calculations). Relevant data for $Fe(CO)_5$,[77] $Cr(CO)_6$,[78] and $Mn(CO)_5Br$[79] are given in Table IV. In each case the M–C–O bending modes are significantly higher in frequency than the M–C stretches. This behavior is, of course, different from that of simpler molecules, for which bending frequencies are typically half those of stretching frequencies. The M–C–O bending force constant is high because of the back-bonding, which dominates the M–C–O linkage and is optimal for a 180° M–C–O angle.

The most direct comparison with heme–CO adducts is provided by the axial carbonyl group in $Mn(CO)_5Br$.[79] Because the trans ligand, Br^-, is not a π-acceptor, back-bonding to the axial carbonyl is stronger than it is to the equatorial carbonyls (or the carbonyl groups of the other compounds listed), which have to share the metal d_π orbitals with one another. Consequently the axial carbonyl group of $Mn(CO)_5Br$ has a higher M–C stretching frequency, 473 cm^{-1}, and a lower C–O stretching frequency, 1992 cm^{-1}, than the others listed. These values are close to the typical values in heme–CO complexes. Likewise, the M–C–O bending

(76) Shimanouchi, T. *Pure Appl. Chem.* **1963**, *7*, 131–145.
(77) Jones, L. H.; McDowell, R. S.; Goldblatt, M.; Swanson, B. I. *J. Chem. Phys.* **1972**, *57*, 2050–2064.
(78) Adams, D. M.; Taylor, I. D. *J. Chem. Soc., Faraday Trans. 2* **1982**, *78*, 1051–1064.
(79) (a) Ottesen, D. K.; Gray, H. B.; Jones, L. H.; Goldblatt, M. *Inorg. Chem.* **1973**, *12*, 1051–1061. (b) Adams, D. M.; Taylor, I. K. *J. Chem. Soc., Faraday Trans. 2* **1982**, *78*, 1065–1090.

Table V. Comparison of Neutron and X-ray Structures of MbCO

Important Metrical Parameters

	neutron	X-ray		neutron	X-ray
Fe–C, Å	2.12[a]	1.92 (2.27[b])	Fe–C–O′, deg	135	141
C–O, Å[c]	1.21	1.20	N_ϵ···O, Å[d]	3.48	3.94
C–O′, Å	1.19	1.17	N_ϵ···O′, Å	2.60	2.66
Fe–C–O, deg	146	120			

Deviation in Positions of Atoms between Neutron (ne) and X-ray (x) Structures

	av (range)		av (range)
Fe porphyrin core[e]	0.17 (0.10–0.39)	O'_{ne}···O'_x, Å	0.30
porphyrin substituents[f]	0.28 (0.13–0.67)	C_{ne}···C_x, Å	0.23
O_{ne}···O_x, Å[g]	0.65		

[a] Neutron data from ref 10, and X-ray data from ref 11. Compare these distances with that of 1.77(2) Å in Fe(TPP)(CO)(py), in ref 82. [b] From an unconstrained refinement. [c] For the two half-oxygens of CO, the atom designated by O has been switched to O′ and vice versa in the X-ray study so as to agree with the notation used in the neutron study. [d] His E7 N_ϵ to CO oxygen distance as shown in Figure 4. [e] Deviation of the 25 atoms comprising the porphyrin core and Fe atom. [f] Deviation of the 14 substituent C atoms on the porphyrin ring. Some of the O atoms of the propionic acid side chain differed by as much as 1.5 Å, and hence no O atoms are included. [g] Distance between positions of indicated atoms in the two structures.

frequency, at 546 cm^{-1}, is near the 560–580-cm^{-1} range of heme–CO adducts in proteins and model compounds.

Tsuboi's overtone proposal offers an alternative explanation for resonance enhancement, since the overtone of any mode is totally symmetric. There are well-established precedents for enhancement of overtones whose fundamentals are weak or missing because of symmetry.[50] This proposal does not, however, explain why enhancement is *absent* for ordinary porphyrin FeCO adducts in solution or in protein adducts that lack distal polar interactions. Activation of the fundamental via symmetry-lowering interactions provides a consistent explanation for all of the data.

These considerations make it clear that the ca. 560-cm^{-1} ^{13}C-sensitive band in the RR spectra of heme proteins and models arises from the FeCO bending mode fundamental and not its overtone.

Appendix 2: Crystallographic Uncertainties

To assess possible errors in CO placement in neutron[10] and X-ray[11] diffraction studies of MbCO, we first refer to the structure determination of poplar plastocyanin,[80] a protein substantially smaller (10.5 kD) than Mb (17 kD). As part of the plastocyanin determination, Guss et al.[80] made a thorough comparison of refinements and refinement strategies with the purpose of assessing accuracy and precision in protein structure analysis. They conclude that uncertainties in the Cu–ligand bond lengths are about 0.05 Å at 1.6-Å resolution and about 0.07 Å at 1.8 Å; the average error in light-atom positions at 1.33-Å resolution is about 0.15 Å, while it is perhaps 0.20 Å at 1.6-Å resolution. For MbCO the average error in the X-ray determination[11] of the C, N, and O positions should be of the order of 0.20 Å, since the resolution was 1.5 Å, while it should be higher, perhaps 0.25 or 0.30 Å, in the neutron study where the resolution is poorer (1.8 Å) and the effective number of variables is greater owing to the significant scattering from deuterium.[81] That these error estimates are reasonable may be seen from a comparison (Table V) of the two structure determinations. The average difference of 0.17 Å for the 25 atoms of the porphyrin core might at first seem smaller than would be expected from the above estimates. However, in both structure determinations the pyrrole groups were separately restrained to be planar and the Fe–N(pyrrole) distances were restrained to be 2.01 Å. In the porphyrin side chains, where there were no restraints, the average positional difference of 0.28 Å is consistent with the above estimates.

Although one would expect the positional error of the half-oxygen atoms (of CO, labeled O and O′ in Figure 4) to be roughly 1.5 times the above values, we can obtain another estimate from geometrical considerations. As discussed above, the neutron study finds no deuterium on the N_ϵ atom of the distal histidine (Figure 4). But the N_ϵ···O′ distance is 2.60 Å (neutrons) or 2.66 Å (X-rays). This distance represents an N···O interaction totally unprecedented in the structural literature: either atom N_ϵ is deuterated and the 2.60-Å distance represents a rather normal N–D···O bond or atoms N_ϵ or O′ or both are badly misplaced. If we accept the placement of deuterons from the neutron diffraction study, then we must conclude that the N_ϵ and O′ or both atoms are misplaced. Since N_ϵ is part of a His group whose geometry was fixed in the refinements, most of the misplacement must lie with the O′ (and O) atoms. This misplacement must be of the order of 0.4 Å in order to lead to a normal N···O distance of 3.1 Å. This error estimate is also consistent with the differences in placement of the O atoms between the neutron and X-ray studies (Table V).

If we now take estimated positional errors of 0.25, 0.25, and 0.40 Å for the Fe, C, and half-O atoms in the neutron determination, we obtain an estimated error of 27° in the FeCO angle; a similar calculation with positional errors of 0.05, 0.20, and 0.40 Å for the Fe, C, and half-O in the X-ray determination leads to an estimated error of 24°. Thus, the average FeCO angles, 140 ± 27° (neutron) or 130 ± 24° (X-ray), do not differ significantly from the nearly linear values obtained in model compounds (Table II),[12,13,82] in HbCO,[15] or in the recent X-ray structure of MbCO.[14]

(80) Guss, J. M.; Bartunik, H. D.; Freeman, H. C. *Acta Crystallogr.* **1992**, *B48*, 790–811.

(81) This estimate ignores the small differences in scattering of X-rays for C, N, and O. For neutrons the differences among the coherent scattering cross sections for Fe, O, N, C, and D (0.95, 0.58, 0.60, 0.66, and 0.67 barns, respectively) are ignored.

(82) Peng, S.-M.; Ibers, J. A. *J. Am. Chem. Soc.* **1976**, *98*, 8032–8036.

(83) Yoshida, Z.; Sugimoto, H.; Ogoshi, H. *Adv. Chem. Ser.* **1980**, *No. 191*, 307.

(84) (a) Chottard, G.; Schappacher, M.; Ricard, L.; Weiss, R. *Inorg. Chem.* **1984**, *23*, 4557–4561. (b) Schappacher, M.; Ricard, L.; Weiss, R.; Montiel-Monotoya, R.; Gonser, U.; Bill, E.; Trautwein, A. *Inorg. Chim. Acta* **1983**, *78*, L9–L12.

(85) Scheidt, W. R.; Haller, K. J.; Fons, M.; Mashiko, T.; Reed, C. A. *Biochemistry* **1981**, *20*, 3653–3657.

(86) (a) SHELXTL PLUS 4.21 for Siemens Crystallographic Research Systems. G. M. Sheldrick, University of Goettingen, Germany, and Siemens Analytical X-ray Instruments, Inc., Madison, WI, 1990. All computations were performed on a MicroVAX computer. (b) Allen, F. H.; Davies, J. E.; Galloy, J. J.; Johnson, O.; Kennard, O.; Macrae, C. F.; Mitchell, E. M.; Mitchell, G. F.; Smith, J. M.; Watson, D. G. *J. Chem. Inf. Comput. Sci.* **1991**, *31*, 187–204.